

DYNAMIC ANALYSIS OF
AXISYMMETRIC PILE GROUPS

by

Thomas R. Tyson
B.S. Carnegie-Mellon University
(1981)

Submitted to the Department of
Civil Engineering
in Partial Fulfillment of the
Requirements of the
Degree of

MASTER OF SCIENCE IN
CIVIL ENGINEERING

at the

MASSACHUSETTS INSTITUTE OF TECHNOLOGY

May 1983

© Massachusetts Institute of Technology 1983

Signature redacted

Signature of Author _____
Department of Civil Engineering
February 7, 1983

Signature redacted

Certified by _____
Thesis Supervisor

Signature redacted

Accepted by _____
Chairman, Department Committee

Archives

MASSACHUSETTS INSTITUTE
OF TECHNOLOGY

JUL 12 1983

LIBRARIES

DYNAMIC ANALYSIS OF
AXISYMMETRIC PILE GROUPS

by

THOMAS R. TYSON

Submitted to the Department of Civil Engineering
on February 7, 1983 in partial fulfillment of the
requirements for the Degree of Master of Science in
Civil Engineering

ABSTRACT

A method has been formulated for the dynamic analysis of axisymmetric pile groups by expressing the displacement components as a Fourier expansion in the azimuth. The method is then implemented in a previously developed program for the analysis of cylindrical foundations embedded in layered media, based on a finite element formulation.

Numerical verification of the method is achieved by a comparison with the analysis of a 4×4 pile group based on three dimensional continuum theory. Analyses are presented investigating the effects of embedment on the dynamic behavior of pile groups. It is determined that the dynamic stiffness for horizontal and torsional excitation increase substantially more than those for vertical and rocking excitation, with embedment.

Thesis Supervisor: Dr. Eduardo Kausel

Title: Associate Professor of Civil Engineering

ACKNOWLEDGMENTS

The author wishes to express his gratitude to Prof. Eduardo Kausel for his guidance, patience and support. Thanks are also given to Ruth Fletcher for her assistance with the typing and the graduate students in room 1-245 who provided the proper diversions at the right times.

Special thanks go to the unknown secretary who made it possible for the proper greek symbols to be added to the text at the right time.

TABLE OF CONTENTS

	<u>Page</u>
Abstract	2
Acknowledgments	3
Table of Contents	4
1-Introduction	
1.1 Background	5
1.2 Problem and Solution Approach	7
2-Formulation of Method	
2.1 Piles in Cylindrical Coordinates (Waas' Model)	11
2.2 Pile Element Stiffness Matrix	14
2.3 Pile Element Consistent Mass Matrix	17
2.4 Pile Ring Stiffnesses and Masses	18
3-Implementation of Method	
3.1 Introduction	29
3.2 Program BIAX	29
3.3 Extending BIAX for Pile Rings	31
4-Results	
4.1 Introduction	40
4.2 Dynamic Stiffnesses of Pile Groups	41
4.2.1 Verification of Numerical Solution Scheme	41
4.2.2 Embedded versus Non- embedded Pile Foundations	46
4.3 Seismic Response of Pile Groups	56
5-Conclusions	58
Appendix - Pile Element Stiffnesses	60
Bibliography	67

CHAPTER 1 - INTRODUCTION

1.1 Background

The construction of nuclear power plants and offshore structures in the past few decades has generated a need to analyse piles and pile groups subject to dynamic loading. This need has resulted in a considerable amount of research.

Most of the research on pile foundations in the past, has dealt with static behavior (installation effects, ultimate load capacity and settlement, lateral resistance and deflection). The theory of beams on elastic foundations has been the most commonly used method of analysis because of its simplicity, versatility and the fact that it gives reasonable results when adequate values are used for the coefficient of subgrade reaction. More rigorous and advanced solution schemes based on the application of Mindlin's fundamental solution for a point load in the interior of a semi-infinite elastic solid have been developed by Poulos (11, 12, 13) and Benerjee (2, 3). These studies have demonstrated some important factors on the behavior of pile groups, such as the dependence of pile group stiffness on the spacing of the piles, their rigidity and length, the distribution of loads on the cap, as well as the material properties of both

the soil and piles.

More recent research has dealt with the dynamic behavior of piles. While the earlier studies were primarily focussed on the dynamic response of single piles, there are now studies dealing with the behavior of pile groups. Wolf and Von Arx (15) used an axisymmetric finite element formulation to obtain Green's functions for ring loads, which were then used to form the soil flexibility matrix. Nogami (9) used an analytical solution for the problem of axisymmetric vibration in a uniform soil stratum underlain by rigid bedrock, and later extended the solution to layered soil strata (10). Waas and Hartman (14) used the general methodology of Wolf and Von Arx, and developed an efficient scheme for the computation of the Green's functions for ring loads in the analysis of an axisymmetric arrangement of piles. Most recently, Kaynia (8) formulated the problem using three-dimensional continuum theory. Kaynia obtained results for a variety of pile-soil configurations and verified the validity of an approximate method of analysis for a situation involving dynamic loads proposed by Poulos.

These studies have resulted in a few general conclusions about dynamic behavior of pile groups: the behavior of pile groups depends very much on the frequency; the spacing and number of piles have a considerable effect on the dynamic stiffness, but only a minor effect on lateral seismic response; and the interaction effects are stronger for more flexible soil media.

What is still missing is the analysis of pile foundations with embedded pile rafts. All of the above research deals only with pile foundations with rafts at grade level. When the pile foundation has a raft that is below the grade level, the embedment can have a substantial effect on the stiffness of the pile group, primarily because of the confining of the peripheral piles due to the overburden.

1.2 Problem and Solution Approach

Consider the embedded foundation shown in figure 1.1 which is assumed to exhibit cylindrical symmetry. The foundation may or may not be in contact with the surrounding soil; in addition, it is supported by a group of floating or end bearing piles (of circular cross section) in concentric arrangements (fig. 1.2).

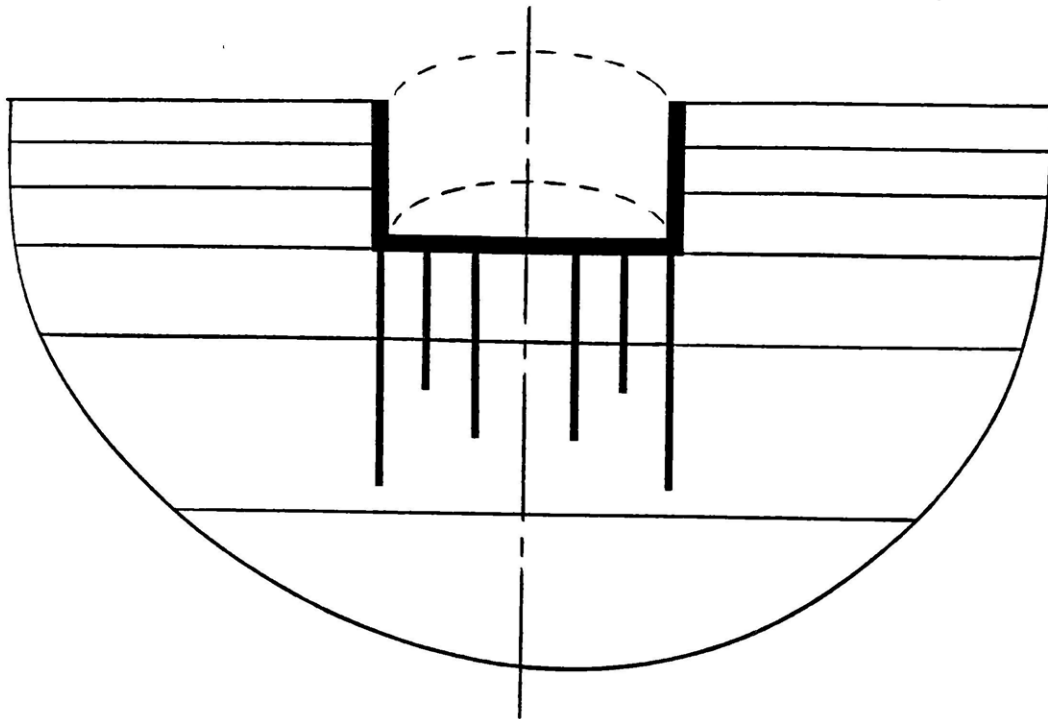


Figure 1.1 Embedded Foundation in a Layered Soil
with Concentric Pile Groups

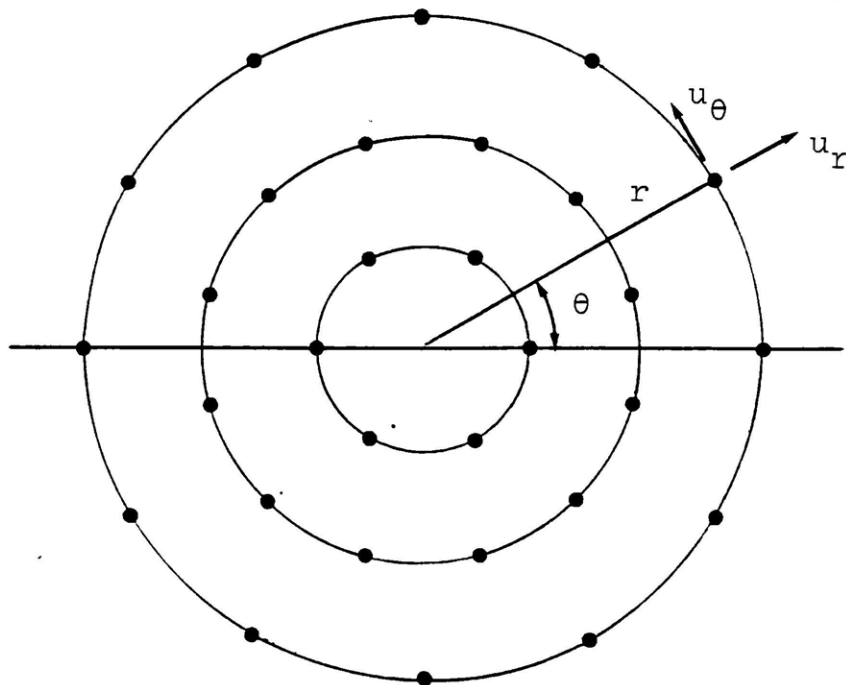


Figure 1.2 Concentric Pile Groups with
Displacement Components

Within each ring, the piles are assumed to be identical (in length, diameter and stiffness) and spaced at regular intervals; however, the piles may change from ring to ring. Following the seminal work by Waas (14), we assume that the displacement components for the piles in each ring may be described by Fourier series in the azimuth, an assumption that parallels the techniques used for solids of revolution, and results in a very efficient solution for the problem at hand.

This appears to be an eminently sound approximation, for if the piles were standing alone (without soil) and the pile cap were given a prescribed displacement or rotation, the displacements along the length of the piles would satisfy the above expansion exactly. On the other hand, if the soil were considered alone, without the piles, it would also satisfy such an expansion because of its cylindrical geometry. In the combined soil-pile configuration, however, this no longer holds exactly, because the soil reactions are concentrated at discrete points in the rings; nevertheless, if the angular distance between the piles in each ring is not large, one may replace the concentrated forces by equivalent distributed tractions along the ring that

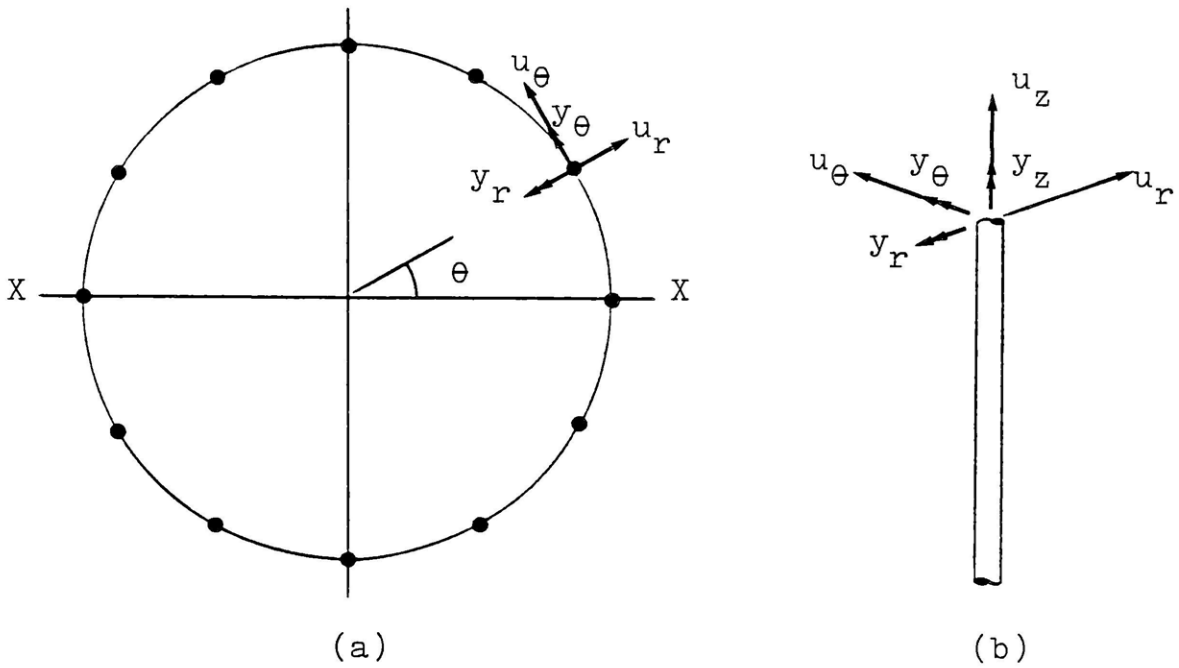
vary smoothly with the azimuth; this substitution, in turn ensures the applicability of the expansion proposed above to the problem of concentric pile arrangements.

This thesis presents the full development of the method along the lines described in the previous paragraphs, and its implementation into a program developed for the analysis of cylindrical foundations embedded in layered media, based on a finite element formulation. The approach is verified by using a case presented by Kaynia for a 4 x 4 pile group, and then the effect of embedment is investigated using a soil-pile system compatible with a nuclear containment structure.

CHAPTER 2 - Formulation of Method

2.1 Piles in Cylindrical Coordinates (Waas' model)

Consider a ring of piles exhibiting double symmetry and connected to a rigid pile cap (fig. 2.1).

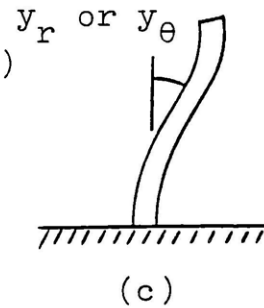


$$\theta = \frac{2\pi}{N} m$$

Where N= Number of piles in Ring

m= Pile number
(numbered sequentially)

Fig.2.1 Pile Ring Configuration
(a) Ring layout (note that there must exist double symmetry).
(b) and (c) sign convention for displacements.



Assume that, within the ring, all of the piles are identical in their lengths, diameters and stiffnesses.

All displacements can be expressed in terms of components about the x-axis. The two components are "symmetric" and "antisymmetric" (see fig. 2.2 and 2.3).

The symmetric component of displacements for any pile in the ring can be expressed as a function of the nominal displacements:

$$\begin{Bmatrix} u_r \\ y_\theta \\ u_\theta \\ y_r \\ u_z \\ y_z \end{Bmatrix}_s = \begin{Bmatrix} \bar{u}_r \cos n\theta \\ \bar{y}_\theta \cos n\theta \\ -\bar{u}_\theta \sin n\theta \\ -\bar{y}_r \sin n\theta \\ \bar{u}_z \cos n\theta \\ -\bar{y}_z \sin n\theta \end{Bmatrix} \quad (2.1)$$

where n represents the Fourier mode (which will be either 0 or 1, see section 3.2).

In the same manner the antisymmetric component of displacements for any pile in the ring can be expressed as a function of the nominal displacements:

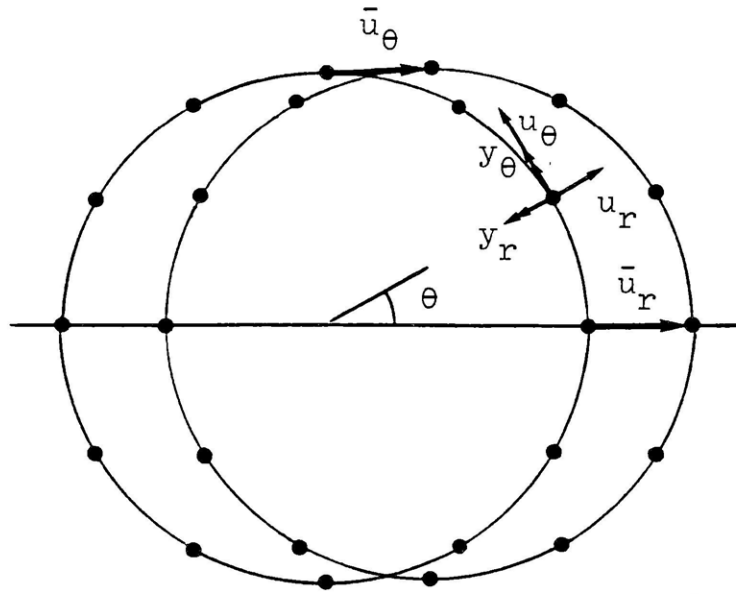


Fig.2.2 Symmetric Component of Displacements

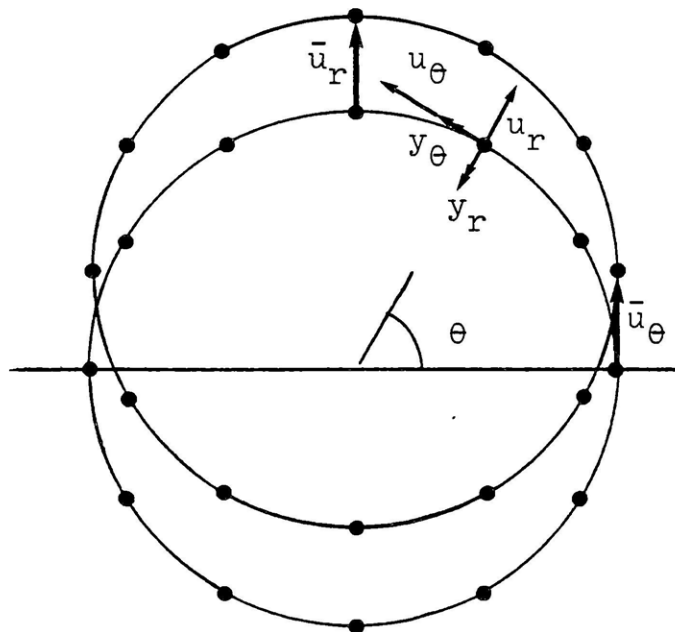


Fig.2.3 Antisymmetric Component of Displacements

$$\begin{Bmatrix} u_r \\ y_\theta \\ u_\theta \\ y_r \\ u_z \\ y_z \end{Bmatrix}_a = \begin{Bmatrix} \bar{u}_r \sin n\theta \\ \bar{y}_\theta \sin n\theta \\ \bar{u}_\theta \cos n\theta \\ \bar{y}_r \cos n\theta \\ \bar{u}_z \sin n\theta \\ \bar{y}_z \cos n\theta \end{Bmatrix} \quad (2.2)$$

Similar expressions hold also for the forces:

$$\begin{Bmatrix} V_r \\ M_\theta \\ V_\theta \\ M_r \\ V_z \\ M_z \end{Bmatrix}_s = \begin{Bmatrix} \bar{V}_r \cos n\theta \\ \bar{M}_\theta \cos n\theta \\ -\bar{V}_\theta \sin n\theta \\ -\bar{M}_r \sin n\theta \\ \bar{V}_z \cos n\theta \\ -\bar{M}_z \sin n\theta \end{Bmatrix} ; \begin{Bmatrix} V_r \\ M_\theta \\ V_\theta \\ M_r \\ V_z \\ M_z \end{Bmatrix}_a = \begin{Bmatrix} \bar{V}_r \sin n\theta \\ \bar{M}_\theta \sin n\theta \\ \bar{V}_\theta \cos n\theta \\ \bar{M}_r \cos n\theta \\ \bar{V}_z \sin n\theta \\ \bar{M}_z \cos n\theta \end{Bmatrix} \quad (2.3)$$

2.2 Pile Element Stiffness Matrix

Consider now a pile element of length L (fig.2.4).

The relationship between the forces and displacements is:

$$\begin{Bmatrix} V_r^a \\ M_\theta^a \\ V_r^b \\ M_\theta^b \end{Bmatrix} = \begin{bmatrix} K_{aa} & K_{ab} \\ K_{ba} & K_{bb} \end{bmatrix} \begin{Bmatrix} u_r^a \\ y_\theta^a \\ u_r^b \\ y_\theta^b \end{Bmatrix} \quad (2.4a)$$

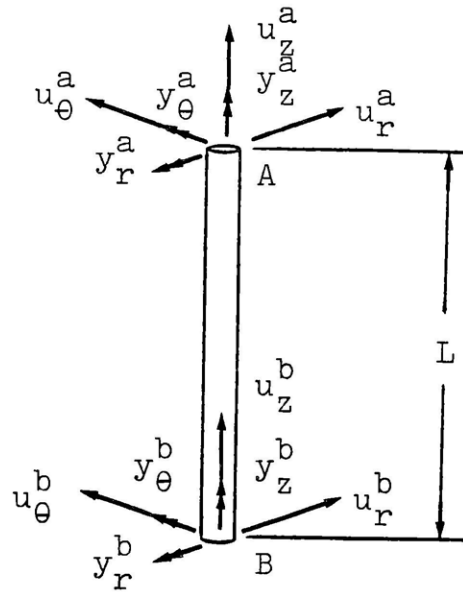


Figure 2.4 Pile Element
Sign Convention

$$\begin{Bmatrix} V_{\theta}^a \\ M_r^a \\ V_{\theta}^b \\ M_r^b \end{Bmatrix} = \begin{bmatrix} K_{aa} & K_{ab} \\ K_{ba} & K_{bb} \end{bmatrix} \begin{Bmatrix} u_{\theta}^a \\ y_r^a \\ u_{\theta}^b \\ y_r^b \end{Bmatrix} \quad (2.4b)$$

$$\begin{Bmatrix} V_z^a \\ V_z^b \end{Bmatrix} = \frac{EA}{L} \begin{bmatrix} 1 & -1 \\ -1 & 1 \end{bmatrix} \begin{Bmatrix} u_z^a \\ u_z^b \end{Bmatrix} \quad (2.4c)$$

$$\begin{Bmatrix} M_z^a \\ M_z^b \end{Bmatrix} = \frac{GJ}{L} \begin{bmatrix} 1 & -1 \\ -1 & 1 \end{bmatrix} \begin{Bmatrix} y_z^a \\ y_z^b \end{Bmatrix} \quad (2.4d)$$

where, for the sign convention used, the elements of the stiffness matrix are:

$$K_{aa} = \begin{bmatrix} v' - \frac{6P}{5L} & -\frac{L}{2} v' + \frac{P}{10} \\ -\frac{L}{2} v' + \frac{P}{10} & \frac{EI}{L} + \frac{L^2}{4} v' - \frac{4}{30} PL \end{bmatrix}$$

$$K_{ab} = K_{ba}^T = \begin{bmatrix} -v' + \frac{6P}{5L} & -\frac{L}{2} v' + \frac{P}{10} \\ \frac{L}{2} v' - \frac{P}{10} & -\frac{EI}{L} + \frac{L^2}{4} v' + \frac{PL}{30} \end{bmatrix}$$

$$K_{bb} = \begin{bmatrix} v' - \frac{6P}{5L} & \frac{L}{2} v' - \frac{P}{10} \\ \frac{L}{2} v' - \frac{P}{10} & \frac{EI}{L} + \frac{L^2}{4} v' - \frac{4PL}{30} \end{bmatrix}$$

where

$$v' = \left(\frac{L^3}{12EI} + \frac{\lambda L}{GA} \right)^{-1}$$

P = axial load on the pile element

L = length of pile element

E = modulus of elasticity of pile element

I = moment of inertia of pile cross section

G = shear modulus of pile element

A = area of pile cross section

λ = shape factor relating gross area to shear area ($\lambda = 7/6$ for circular cross sections)

These stiffnesses include bending and shear effects, plus a term reflecting the geometric nonlinearity due to the axial load. The appendix includes the derivation of the stiffnesses.

2.3 Pile Element Consistent Mass Matrix

The consistent mass matrix for a beam element is well known and need not be elaborated on here. The matrix is given here for reference only, using the present sign convention as presented in figure 2.4.

The complete consistent mass matrix is:

$$\begin{Bmatrix} V_r^a \\ M_\theta^a \\ V_r^b \\ M_\theta^b \end{Bmatrix} = \begin{bmatrix} M_{aa} & M_{ab} \\ M_{ba} & M_{bb} \end{bmatrix} \begin{Bmatrix} \ddot{u}_r^a \\ \ddot{y}_\theta^a \\ \ddot{u}_r^b \\ \ddot{y}_\theta^b \end{Bmatrix}$$

$$\begin{Bmatrix} V_\theta^a \\ M_r^a \\ V_\theta^b \\ M_r^b \end{Bmatrix} = \begin{bmatrix} M_{aa} & M_{ab} \\ M_{ba} & M_{bb} \end{bmatrix} \begin{Bmatrix} \ddot{u}_\theta^a \\ \ddot{y}_r^a \\ \ddot{u}_\theta^b \\ \ddot{y}_r^b \end{Bmatrix}$$

$$\begin{Bmatrix} V_z^a \\ V_z^b \end{Bmatrix} = \frac{m}{6} \begin{bmatrix} 2 & 1 \\ 1 & 2 \end{bmatrix} \begin{Bmatrix} \ddot{u}_z^a \\ \ddot{u}_z^b \end{Bmatrix}$$

$$\begin{Bmatrix} M_z^a \\ M_z^b \end{Bmatrix} = \frac{\rho I_p L}{6} \begin{bmatrix} 2 & 1 \\ 1 & 2 \end{bmatrix} \begin{Bmatrix} \ddot{y}_z^a \\ \ddot{y}_z^b \end{Bmatrix}$$

where

$$M_{aa} = \frac{m}{420} \begin{bmatrix} 156 & -22L \\ -22L & 4L^2 \end{bmatrix}$$

$$M_{ab} = M_{ba}^T = \frac{m}{420} \begin{bmatrix} 54 & 13L \\ -13L & -3L^2 \end{bmatrix}$$

$$M_{bb} = \frac{m}{420} \begin{bmatrix} 156 & 22L \\ 22L & 4L^2 \end{bmatrix} .$$

2.4 Pile Ring Stiffnesses and Masses

To find the stiffness matrix for a ring of pile elements, define the transformation matrix, T , such that

$$U = T\bar{U} \quad (2.5)$$

$$\begin{Bmatrix} u_1 \\ u_2 \\ \vdots \\ u_N \end{Bmatrix} = \begin{bmatrix} t_1 & & & \\ & t_2 & & \\ & & \ddots & \\ & & & t_N \end{bmatrix} \begin{Bmatrix} \bar{u}_1 \\ \bar{u}_2 \\ \vdots \\ \bar{u}_N \end{Bmatrix}$$

For the symmetric component of displacements, this is

$$\begin{Bmatrix} u_r \\ y_\theta \\ u_\theta \\ y_r \\ u_z \\ y_z \end{Bmatrix} = \begin{bmatrix} \cos n\theta & & & & & \\ & \cos n\theta & & & & \\ & & -\sin n\theta & & & \\ & & & -\sin n\theta & & \\ & & & & \cos n\theta & \\ & & & & & -\sin n\theta \end{bmatrix} \begin{Bmatrix} \bar{u}_r \\ \bar{y}_\theta \\ \bar{u}_\theta \\ \bar{y}_r \\ \bar{u}_z \\ \bar{y}_z \end{Bmatrix}$$

Taking the stiffness equations, substitute equation 2.5,

$$P = KU = KT\bar{U} \quad (2.6)$$

and premultiply both sides by T^T ,

$$P_{\text{mod}} = T^T P = T^T K T \bar{U} = K_o \bar{U} \quad (2.7)$$

where

$$K_o = T^T K T. \quad (2.8)$$

Since T is a diagonal matrix the elements of K_o are represented simply by

$$k_{o_{ij}} = k_{ij} \sum t_i t_j. \quad (2.9)$$

The elements of the transformation matrix can have one of three values

$$t_i = \begin{cases} \cos n \frac{2\pi}{N} m \\ \sin n \frac{2\pi}{N} m \\ -\sin n \frac{2\pi}{N} m \end{cases} .$$

Therefore, the summation term in equation 2.9 will have one of three values

$$t_i t_j = \begin{cases} \sum_{m=1}^N \cos^2 n \frac{2\pi}{N} m \\ \sum_{m=1}^N \sin^2 n \frac{2\pi}{N} m \\ \sum_{m=1}^N \pm \sin n \frac{2\pi}{N} m \cos n \frac{2\pi}{N} m \end{cases}$$

where N is the number of piles in the ring. For $n=0$ these terms reduce to

$$\sum_{m=1}^N \cos^2 (0) = N$$

$$\sum_{m=1}^N \sin^2 (0) = 0$$

$$\sum_{m=1}^N \sin (0) \cos (0) = 0 .$$

For $n=1$ these terms reduce to

$$\sum_{m=1}^N \cos^2 \frac{2\pi}{N} m = N/2 \quad \text{for } N > 2$$

$$\sum_{m=1}^N \sin^2 \frac{2\pi}{N} m = N/2 \quad \text{for } N > 2$$

$$\sum_{m=1}^N \sin \frac{2\pi}{N} m \cos \frac{2\pi}{N} m = 0 \quad .$$

For convenience, the following notation will be used throughout the rest of the paper:

$$C^2 = \sum_{m=1}^N \cos^2 n \frac{2\pi}{N} m = \begin{cases} N & \text{for } n=0 \\ N/2 & \text{for } n=1 \end{cases}$$

$$S^2 = \sum_{m=1}^N \sin^2 n \frac{2\pi}{N} m = \begin{cases} 0 & \text{for } n=0 \\ N/2 & \text{for } n=1 \end{cases} \quad .$$

Reordering the displacement components in the stiffness equations 2.4, and modifying according to equation 2.7 yields, for the symmetric component,

$$\begin{Bmatrix} v_r^a \\ v_r^b \\ M_\theta^a \\ M_\theta^b \end{Bmatrix} = C^2 \begin{bmatrix} K_{VV} & K_{VM} \\ K_{MV} & K_{MM} \end{bmatrix} \begin{Bmatrix} u_r^a \\ u_r^b \\ y_\theta^a \\ y_\theta^b \end{Bmatrix} \quad (2.10a)$$

$$\begin{Bmatrix} v_{\theta}^a \\ v_{\theta}^b \\ M_r^a \\ M_r^b \end{Bmatrix} = S^2 \begin{bmatrix} K_{VV} & K_{VM} \\ K_{MV} & K_{MM} \end{bmatrix} \begin{Bmatrix} u_{\theta}^a \\ u_{\theta}^b \\ y_r^a \\ y_r^b \end{Bmatrix} \quad (2.10b)$$

$$\begin{Bmatrix} v_z^a \\ v_z^b \end{Bmatrix} = \frac{EA}{L} C^2 \begin{bmatrix} 1 & -1 \\ -1 & 1 \end{bmatrix} \begin{Bmatrix} u_z^a \\ u_z^b \end{Bmatrix} \quad (2.10c)$$

$$\begin{Bmatrix} M_z^a \\ M_z^b \end{Bmatrix} = \frac{GJ}{L} S^2 \begin{bmatrix} 1 & -1 \\ -1 & 1 \end{bmatrix} \begin{Bmatrix} y_z^a \\ y_z^b \end{Bmatrix} \quad (2.10d)$$

where

$$K_{VV} = \begin{bmatrix} v' - \frac{6P}{5L} & -v' + \frac{6P}{5L} \\ -v' + \frac{6P}{5L} & v' - \frac{6P}{5L} \end{bmatrix}$$

$$K_{VM} = K_{MV}^T = \begin{bmatrix} -\frac{L}{2} v' + \frac{P}{10} & -\frac{L}{2} v' + \frac{P}{10} \\ \frac{L}{2} v' - \frac{P}{10} & \frac{L}{2} v' - \frac{P}{10} \end{bmatrix}$$

$$K_{MM} = \begin{bmatrix} \frac{EI}{L} + \frac{L^2}{4} v' - \frac{4}{30} PL & -\frac{EI}{L} + \frac{L^2}{4} v' + \frac{PL}{30} \\ -\frac{EI}{L} + \frac{L^2}{4} v' + \frac{PL}{30} & \frac{EI}{L} + \frac{L^2}{4} v' - \frac{4}{30} PL \end{bmatrix}$$

The same formulation holds for the mass matrix as for the stiffness matrix, above. Formulating the mass matrix in this way yields

$$\begin{Bmatrix} v_r^a \\ v_r^b \\ M_\theta^a \\ M_\theta^b \end{Bmatrix} = C^2 \begin{bmatrix} M_{VV} & M_{VM} \\ M_{MV} & M_{MM} \end{bmatrix} \begin{Bmatrix} \ddot{u}_r^a \\ \ddot{u}_r^b \\ \ddot{y}_\theta^a \\ \ddot{y}_\theta^b \end{Bmatrix} \quad (2.11a)$$

$$\begin{Bmatrix} v_\theta^a \\ v_\theta^b \\ M_r^a \\ M_r^b \end{Bmatrix} = S^2 \begin{bmatrix} M_{VV} & M_{VM} \\ M_{MV} & M_{MM} \end{bmatrix} \begin{Bmatrix} \ddot{u}_\theta^a \\ \ddot{u}_\theta^b \\ \ddot{y}_r^a \\ \ddot{y}_r^b \end{Bmatrix} \quad (2.11b)$$

$$\begin{Bmatrix} v_z^a \\ v_z^b \end{Bmatrix} = C^2 m \begin{bmatrix} 1/3 & 1/6 \\ 1/6 & 1/3 \end{bmatrix} \begin{Bmatrix} \ddot{u}_z^a \\ \ddot{u}_z^b \end{Bmatrix} \quad (2.11c)$$

$$\begin{Bmatrix} M_z^a \\ M_z^b \end{Bmatrix} = S^2 \frac{mr^2}{12} \begin{bmatrix} 2 & 1 \\ 1 & 2 \end{bmatrix} \begin{Bmatrix} \ddot{y}_z^a \\ \ddot{y}_z^b \end{Bmatrix} \quad (2.11c)$$

where

r = radius of pile element

m = mass of pile element

and

$$\begin{aligned}
 M_{VV} &= \frac{m}{420} \begin{bmatrix} 156 & 54 \\ 54 & 156 \end{bmatrix} \\
 M_{VM} &= M_{MV}^T = \frac{m}{420} \begin{bmatrix} -22L & 13L \\ -13L & 22L \end{bmatrix} \\
 M_{MM} &= \frac{m}{420} \begin{bmatrix} 4L^2 & -3L^2 \\ -3L^2 & 4L^2 \end{bmatrix} .
 \end{aligned}$$

Assembling n pile elements into the ring matrices yields a simple matrix of a general form for either stiffness or mass:

$$P_{\text{mod}} = h \times \begin{bmatrix} Q & R \\ R & S \end{bmatrix} \begin{Bmatrix} \underline{u} & \text{or} & \underline{\ddot{u}} \\ \underline{v} & & \underline{\ddot{v}} \end{Bmatrix} \quad (2.12)$$

where

$$\begin{aligned}
 h &= C^2 \text{ for displacement vector } \begin{Bmatrix} \underline{u}_r \\ \underline{v}_\theta \end{Bmatrix} \text{ or} \\
 &\text{acceleration vector } \begin{Bmatrix} \underline{\ddot{u}}_r \\ \underline{\ddot{v}}_\theta \end{Bmatrix} \\
 h &= S^2 \text{ for displacement vector } \begin{Bmatrix} \underline{u}_\theta \\ \underline{v}_r \end{Bmatrix} \text{ or} \\
 &\text{acceleration vector } \begin{Bmatrix} \underline{\ddot{u}}_\theta \\ \underline{\ddot{v}}_r \end{Bmatrix}
 \end{aligned}$$

Q is a matrix of the form

$$U_i = -\frac{E_i I_i}{L_i} + \frac{L_i^2}{4} V_i' - \frac{P_i L_i}{30}$$

where

$$V_i' = \left(\frac{L_i^3}{12E_i I_i} + \frac{\lambda L_i}{G_i A_i} \right)^{-1}$$

then

$$A(1) = R_1$$

$$A(i) = R_{i-1} + R_i$$

$$A(n+1) = R_n$$

$$B(i) = -R_i$$

$$C(1) = S_1$$

$$C(i) = S_i - S_{i-1}$$

$$C(n+1) = -S_n$$

$$D(i) = S_i$$

$$E(1) = T_1$$

$$E(i) = T_i + T_{i-1}$$

$$E(n+1) = T_n$$

$$F(i) = U_i \quad .$$

For the mass matrix let

$$R_i = \frac{156}{420} m_i$$

$$S_i = \frac{-22}{420} m_i$$

$$T_i = \frac{4L_i^2}{420} m_i$$

then

$$\begin{aligned}
 A(1) &= R_1 \\
 A(i) &= R_i + R_{i-1} \\
 A(n+1) &= R_n \\
 B(i) &= \frac{54}{420} m_i \\
 C(1) &= S_1 \\
 C(i) &= S_i - S_{i-1} \\
 C(n+1) &= -S_n \\
 D(i) &= \frac{13L_i}{420} m_i \\
 E(1) &= T_1 \\
 E(i) &= T_i + T_{i-1} \\
 E(n+1) &= T_n \\
 F(i) &= \frac{-3L_i^2}{420} m_i .
 \end{aligned}$$

Assembling the elements for axial translation yields a matrix in the form of Q, above, where if you let

$$S_i = \frac{E_i A_i}{L_i}$$

then

$$\begin{aligned}
 A(1) &= S_1 \\
 A(i) &= S_i + S_{i-1} \\
 A(n+1) &= S_n \\
 B(i) &= -S_i
 \end{aligned}$$

for stiffness. For mass let

$$M_i = \frac{m_i}{3}$$

then

$$A(1) = M_1$$

$$A(i) = M_i + M_{i-1}$$

$$A(n+1) = M_n$$

$$B(i) = M_i/2 .$$

For the antisymmetric component of displacements the formulation is the same, with only the C^2 and S^2 terms being reversed in the results.

The program BIAX, in which this formulation will be implemented, works on up to three degrees of freedom. In BIAX the degrees of freedom R, Z, and θ , correspond to u_r , u_z , and u_θ in this formulation. Therefore, while the assembling of the stiffness and mass matrices for \underline{y}_z follows similarly to \underline{u}_z , above, it is not presented here.

CHAPTER 3 - Implementation of Method

3.1 Introduction

This chapter discusses how the method formulated in the previous chapter is implemented using the program BIAX. The relevant aspects of the program are presented first, then the extensions for the pile ring formulation are discussed.

3.2 Program BIAX

The program BIAX was developed by Kausel (5) for the analysis of cylindrical foundations embedded in layered media. The program, which is based on a finite element formulation, is capable of analyzing problems of either external or seismic excitations, and features a sophisticated transmitting boundary.

BIAX is based on a finite element formulation for the dynamic analysis of axisymmetric foundations resting on, and embedded in, viscoelastic soil layers which in turn rest on a rigid halfspace of rock. The program is capable of handling arbitrary non-axisymmetric loads or displacements, using a Fourier expansion method.

The geometry of the problem is broken into two regions; a finite irregular region bounded by a

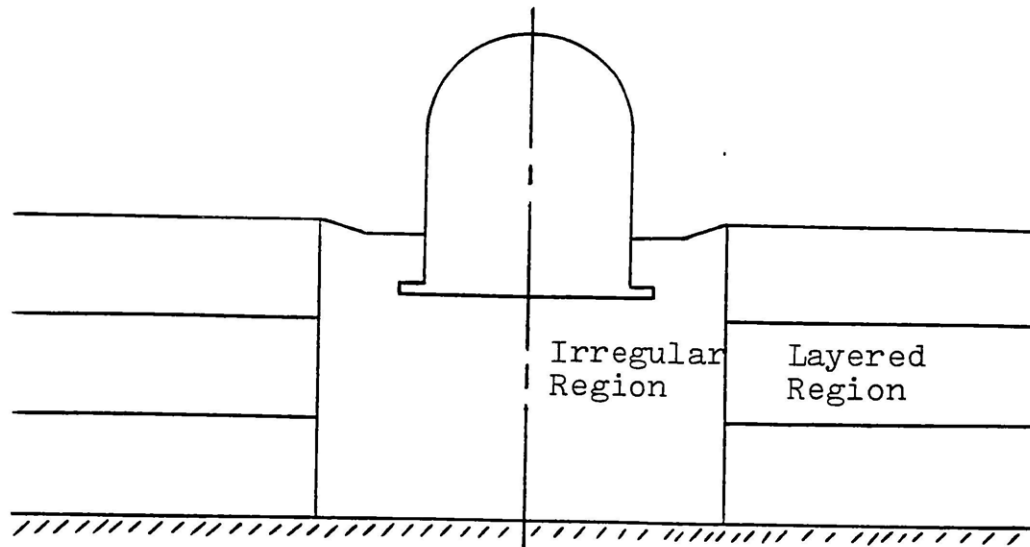


Figure 3.1
Geometry of problem analysed with BIAX

semi-infinite layered far-field region (see fig. 3.1). The irregular region is discretized by means of pseudotridentimensional toroidal finite elements of arbitrary expansion order having three degrees of freedom per nodal ring. The far field is represented by a specially designed consistent energy absorbing boundary, where the dynamic stiffness matrix is expanded in Fourier series about the axis, as are the forces and displacements.

The finite element method performs a pseudo-tridentimensional analysis on solids of revolution by dividing the problem into a number of uncoupled two dimensional problems, and representing the unsymmetric loading or displacements by an equivalent Fourier series about the axis. The three dimensional

nature of the problem is preserved by using three degrees of freedom per nodal ring (u_r , u_z , u_θ). Since the Fourier series exhibits orthogonality, each term in the loading series produces a displacement set in the same Fourier mode as the prescribed loading or displacements. If the prescribed loads (displacements) do not vary too rapidly around the axis only a few terms in the series may be sufficient for an accurate representation. For the general motions under consideration, BIAX uses only the first two modes in the series. These are $n=0$ for vertical and torsional excitation (axisymmetric modes), and $n=1$ for rocking and swaying (plane-symmetric modes).

3.3 Extending BIAX for pile rings

When the stiffness and mass matrices for pile elements are assembled for the pile ring, only two groups of degrees of freedom are coupled; u_r with v_θ , and u_θ with v_r (see equation 2.12). The axial translation and axial rotation terms are both uncoupled from the other terms. Since BIAX uses only three degrees of freedom (u_r , u_z and u_θ), the other three degrees of freedom in the formulation must be condensed out. Since v_z is uncoupled from the other

displacements it can be left out of the final pile ring matrices. As can be seen in equation 2.12, the stiffness and mass matrices for \underline{u}_r with \underline{v}_θ and \underline{u}_θ with \underline{v}_r are the same, and therefore both can be assembled and have the stiffness matrix condensed as one set.

The resulting pile ring stiffness and mass matrices to be assembled into the global matrices for the finite element mesh are as follows:

$$C^2 \begin{bmatrix} A' \end{bmatrix} \begin{Bmatrix} \underline{u}_r \end{Bmatrix} = \begin{Bmatrix} \underline{v}_r \end{Bmatrix}$$

$$S^2 \begin{bmatrix} A' \end{bmatrix} \begin{Bmatrix} \underline{u}_\theta \end{Bmatrix} = \begin{Bmatrix} \underline{v}_\theta \end{Bmatrix}$$

$$C^2 \begin{bmatrix} B' \end{bmatrix} \begin{Bmatrix} \underline{u}_z \end{Bmatrix} = \begin{Bmatrix} \underline{v}_z \end{Bmatrix}$$

for stiffnesses, and

$$C^2 \begin{bmatrix} C' \end{bmatrix} \begin{Bmatrix} \underline{u}_r \end{Bmatrix} = \begin{Bmatrix} \underline{v}_r \end{Bmatrix}$$

$$C^2 \begin{bmatrix} & \\ & C' \end{bmatrix} \begin{Bmatrix} \underline{u}_\theta \end{Bmatrix} = \begin{Bmatrix} \underline{v}_\theta \end{Bmatrix}$$

$$S^2 \begin{bmatrix} & \\ & D' \end{bmatrix} \begin{Bmatrix} \underline{u}_z \end{Bmatrix} = \begin{Bmatrix} \underline{v}_z \end{Bmatrix}$$

for masses, where

A' - is a $n+1 \times n+1$ stiffness matrix resulting from the condensation of the rotational degrees of freedom from the stiffness matrix in equation 2.12

n - is the number of elements associated with the pile ring

$B', C',$ and C' , are matrices of the general form

$$\begin{bmatrix} A(1) & B(1) & & & & & \\ B(1) & A(2) & \cdot & & & & \\ & \cdot & \cdot & \cdot & & & \\ & & \cdot & \cdot & \cdot & & B(n) \\ & & & & \cdot & & \\ & & & B(n) & A(n+1) & & \end{bmatrix}$$

where \underline{A} is a vector of length $n+1$ containing the diagonal terms, and \underline{B} is a vector of length n containing the off diagonal terms. The elements

of these vectors are specified in equation 2.12.

The result of this condensation is the following uncoupled stiffness equations for the pile ring:

$$P'_r = C^2 K_r U_r$$

$$P'_z = C^2 K_z U_z$$

$$P'_\theta = S^2 K_\theta U_\theta$$

for the symmetric component, and

$$P'_r = S^2 K_r U_r$$

$$P'_z = S^2 K_z U_z$$

$$P'_\theta = C^2 K_\theta U_\theta$$

for the antisymmetric component, where P' is the total load component on the pile ring.

The loads used in the program BIAX are loads per radian, so the stiffness equations must be modified to reflect the proper load vector. If we let P be the load per radian and P' be the total load on the pile ring, the following relationships hold:

$$P_r \int_0^{2\pi} \cos^2 n\theta \, d\theta = P'_r$$

$$P_z \int_0^{2\pi} \cos^2 n\theta \, d\theta = P'_z$$

$$P_\theta \int_0^{2\pi} \sin^2 n\theta \, d\theta = P'_\theta$$

for the symmetric component, and

$$P_r \int_0^{2\pi} \sin^2 n\theta \, d\theta = P'_r$$

$$P_z \int_0^{2\pi} \sin^2 n\theta \, d\theta = P'_z$$

$$P_\theta \int_0^{2\pi} \cos^2 n\theta \, d\theta = P'_\theta$$

for the antisymmetric component.

When $n=1$ these relationships reduce to

$$P_r = P'_r / \pi$$

$$P_z = P'_z / \pi$$

$$P_\theta = P'_\theta / \pi$$

for both components, and with $n=0$

$$P_r = P'_r / 2\pi$$

$$P_z = P'_z / 2\pi$$

$$P_\theta = 0$$

for the symmetric component, and

$$P_r = 0$$

$$P_z = 0$$

$$P_\theta = P'_\theta / 2\pi$$

for the antisymmetric component.

Substituting these relationships into the stiffness equations, and evaluating the constants C^2 and S^2 yields:

For $n=1$

$$P_r = \frac{N}{2\pi} K_r U_r$$

$$P_z = \frac{N}{2\pi} K_z U_z$$

$$P_{\theta} = \frac{N}{2\pi} K_{\theta} U_{\theta}$$

for both components, and for $n=0$

$$P_r = \frac{N}{2\pi} K_r U_r$$

$$P_z = \frac{N}{2\pi} K_z U_z$$

$$P_{\theta} = 0$$

for the symmetric component, and

$$P_r = P_z = 0$$

$$P_{\theta} = \frac{N}{2\pi} K_{\theta} U_{\theta}$$

for the antisymmetric component.

When $n=0$, the non-pile elements in BIAX also have the U_0 term of the stiffness equations uncoupled from the other degrees of freedom, therefore we need not be concerned about the symmetric and antisymmetric components of displacements. We can then implement the stiffness functions for the piles, in all cases, as

$$P_r = \frac{N}{2\pi} K_x U_r$$

$$P_z = \frac{N}{2\pi} K_z U_z \quad (3.1)$$

$$P_{\theta} = \frac{N}{2\pi} K_x U_{\theta}$$

Where N is the number of piles in the ring and

$$K_x = K_r = K_\theta .$$

These relationships are based on the terms C^2 and S^2 which only hold as evaluated for N greater than two. Since it is desirable to be able to use a single pile in the center of the other concentric arrangements of piles we must develop the stiffness function for this special case.

The displacement components for a single pile at the center of the cylindrical coordinate system are

$$u_r = \bar{u}_r = u_\theta = \bar{u}_\theta$$

$$u_z = \bar{u}_z$$

and the stiffness equations are

$$P'_r = K_x U_r$$

$$P'_z = K_z U_z$$

$$P'_\theta = K_x U_\theta$$

for n equal to one or zero. Converting the loads on the pile to loads per radian yields

$$P_r = \frac{1}{2\pi} K_x U_r$$

$$P_z = \frac{1}{2\pi} K_z U_z$$

$$P_\theta = \frac{1}{2\pi} K_x U_\theta$$

which is the same as equation 3.1 for N equal to one.

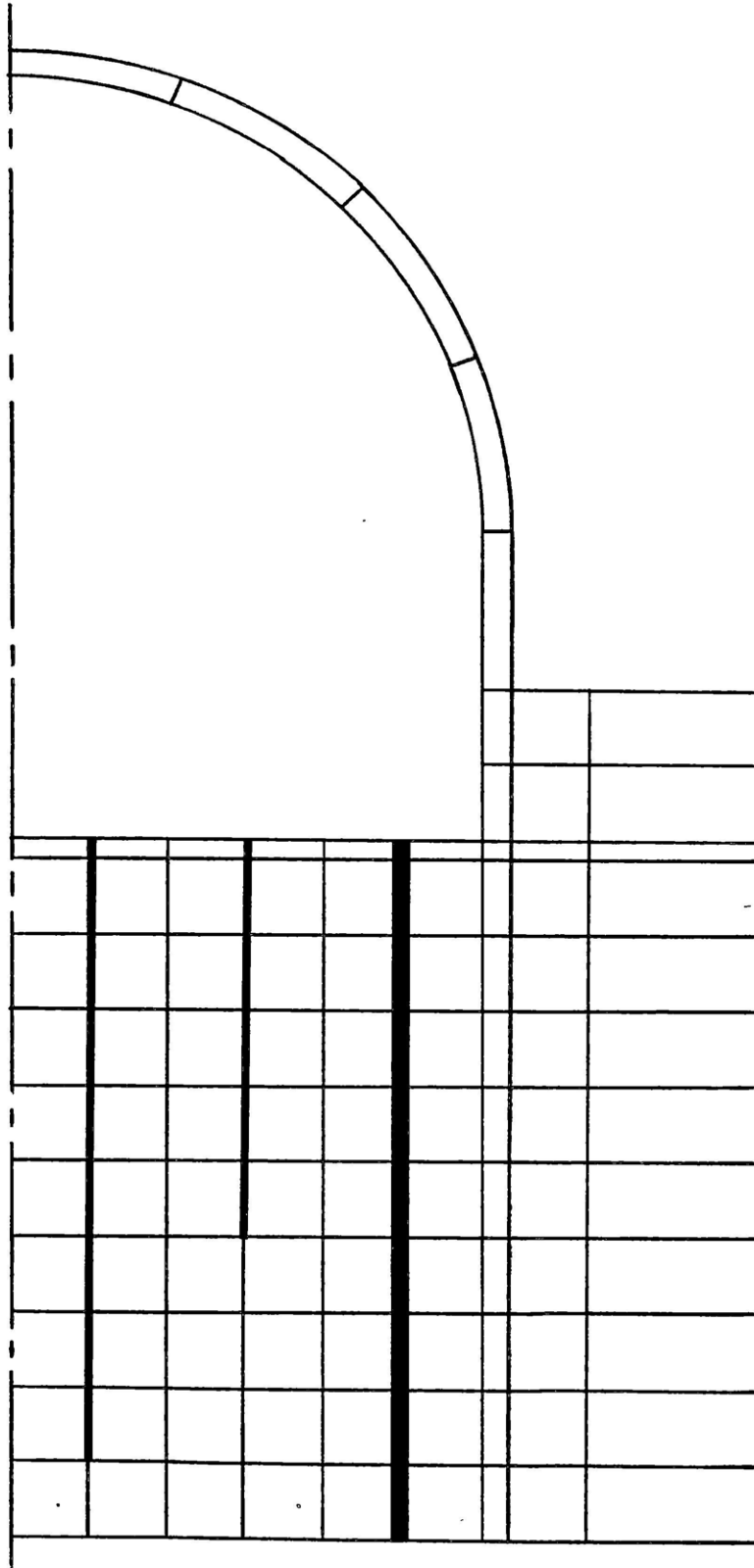


Figure 3.2
Piles in Finite Element Mesh

When the pile ring matrices are assembled with the soil and structural elements, the result is an increase in the stiffness and mass of the soil (structural) elements along the line of the pile (fig. 3.2). The pile ring does not introduce any new nodes or result in the separation of any soil elements. This makes it easy to see that the stiffness of the pile ring, as represented here, results in a continuous cylinder of stiffening material with zero thickness and non-zero mass. This cylinder, along with the Fourier expansion of the loads and displacements, constitutes the method developed here.

Chapter 4 - Results

4.1 Introduction

The objective of this chapter is to present numerical results obtained with the formulation presented in Chapter 2, and to investigate the dynamic behavior of pile groups. There are two quantities of interest in this study: the dynamic stiffnesses of the pile groups corresponding to horizontal, vertical, rocking and torsional modes of vibration; and the seismic response of pile groups. Results are presented to compare with those of Kaynia (8) to verify the validity of the formulation, then results are presented to compare the behavior of embedded pile foundations with non-embedded pile foundations.

The stiffnesses of the pile group, along with the transfer function of the pile cap associated with a seismic excitation, can be used, in the analysis of the superstructure, to account for the foundation-structure interaction effects. A conventional foundation-structure interaction analysis consists of three steps: 1) the foundation stiffnesses (impedances) are computed, to be used as "soil springs" ; 2) the motions of the foundation with a rigid, massless superstructure are

computed (kinematic interaction); 3) the base motions computed in the kinematic interaction step are applied to the structure mounted on the soil springs (inertial interaction).

Throughout this chapter the following notation is used for the material properties of the systems being analyzed:

E = elasticity modulus

G = shear modulus

ρ = mass density

γ = weight density

ν = poisson ratio

β = material damping

C_s = shear wave velocity

ω = frequency of excitation

L = length of pile

d = diameter of pile

s (subscript) = refers to soil

p (subscript) = refers to pile

4.2 Dynamic Stiffnesses of Pile Groups

4.2.1 Verification of Numerical Solution Scheme

In his report, Kaynia (8) has presented the dynamic stiffness functions of various pile groups in a viscoelastic halfspace. The 4 x 4 pile group can be

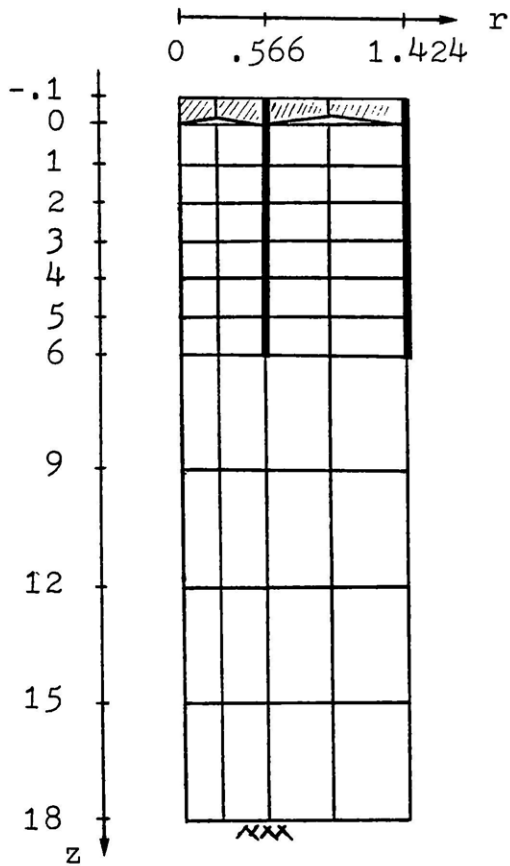


Figure 4.1

Finite element mesh used
for 4 x 4 pile group.

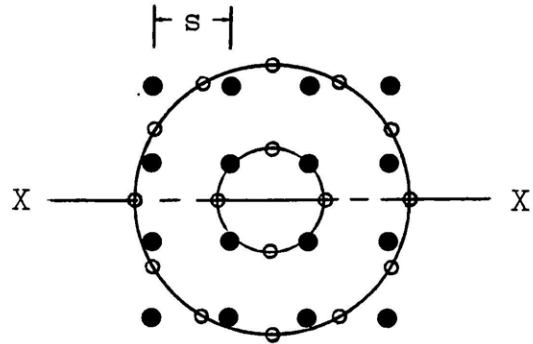


Figure 4.2

Radius of inner ring = $.7075s$
Radius of outer ring = $1.78s$

taken and easily modified to more appropriately fit the requirements of the formulation here, by relocating the piles into two rings, as in figure 4.2, such that the moment of inertia about the x-axis is the same as the original group. This pile arrangement can then be modelled using the finite element mesh as presented in figure 4.1.

The following material and dimensional

specifications are applied to match those used by Kaynia:

$$v_s = 0.40 \quad \beta_s = .05$$

$$v_p = 0.25 \quad \beta_p = .00$$

$$\frac{\rho_s}{\rho_p} = 0.70 \quad \frac{E_s}{E_p} = 10^{-3}$$

$$\frac{s}{d} = 2 \quad \frac{L}{d} = 15$$

Figures 4.3 through 4.6 present the dynamic stiffnesses of the pile group using both Kaynia's results and the method presented here. The notation used in these figures is described below:

$$a_o = \frac{\omega d}{C_s}$$

$k_v(a_o)$ = complex vertical stiffness of the pile group

$k_s(a_o)$ = complex swaying stiffness of the pile group

$k_T(a_o)$ = complex torsional stiffness of the pile group

$k_r(a_o)$ = complex rocking stiffness of the pile group

$k_z^S(a_o=0)$ = complex static vertical stiffness of a single pile

$k_x^S(a_o=0)$ = complex static horizontal stiffness of a single pile

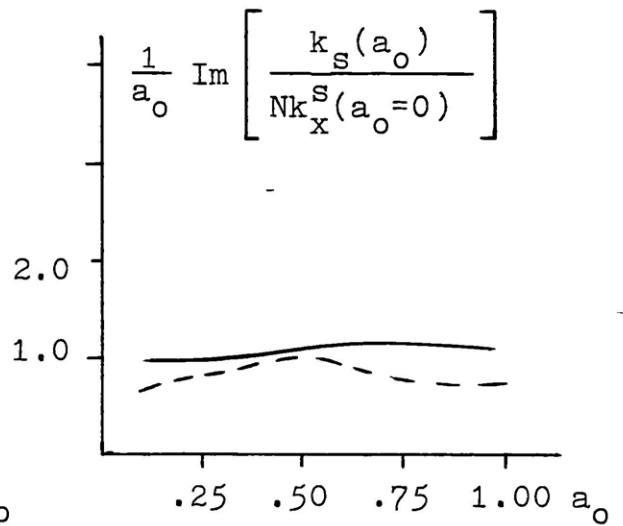
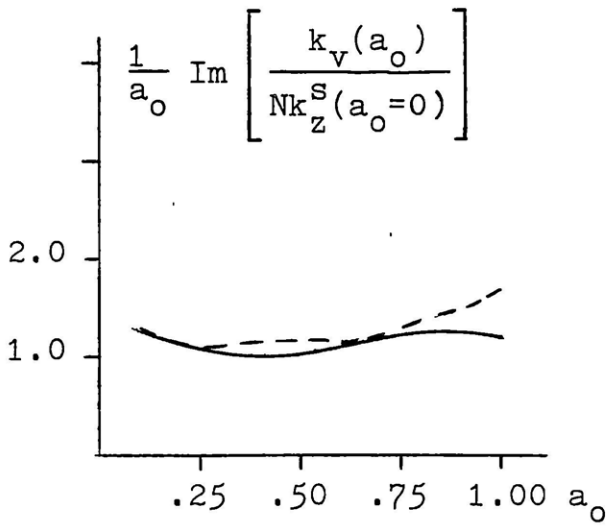
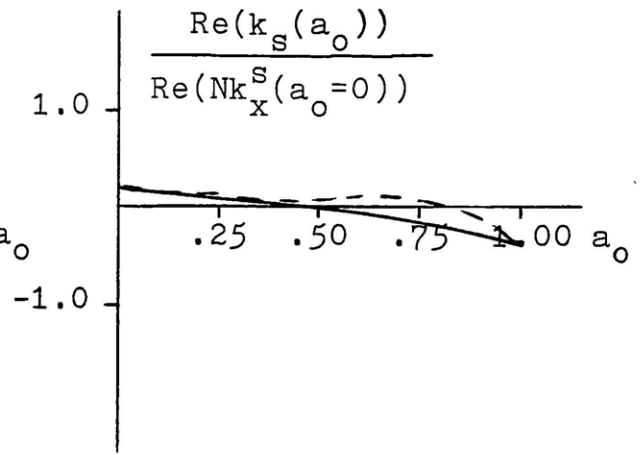
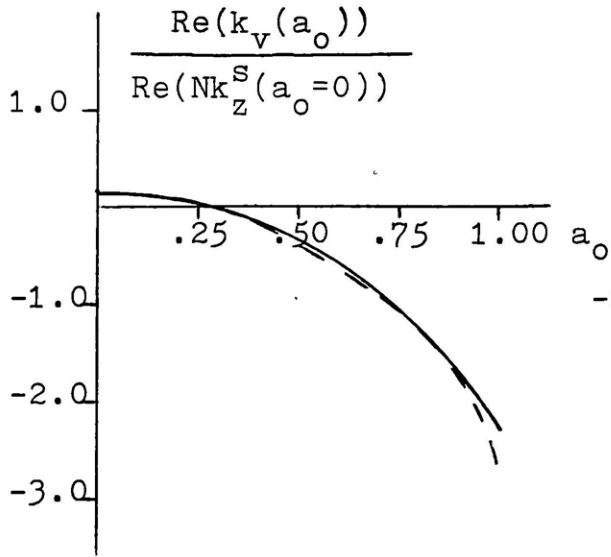


Figure 4.3
Vertical Dynamic Stiffness
of 4 x 4 Pile Group
Solid Line - Kaynia

Figure 4.4
Horizontal Dynamic
Stiffness of 4 x 4
Pile Group
Solid Line - Kaynia

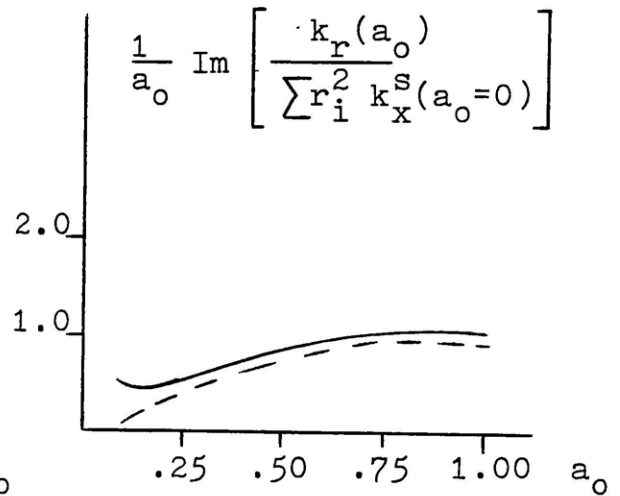
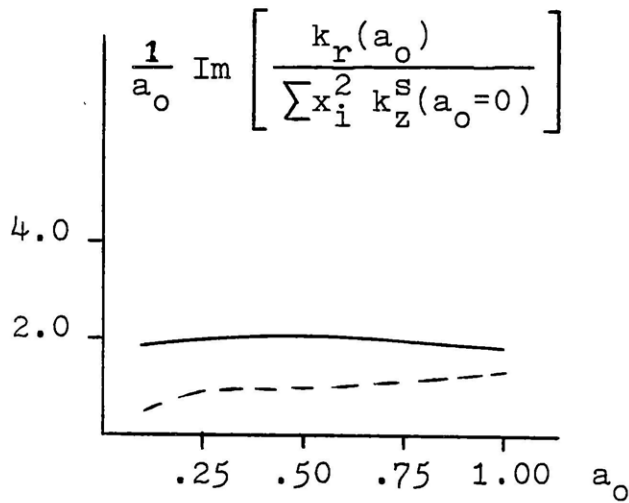
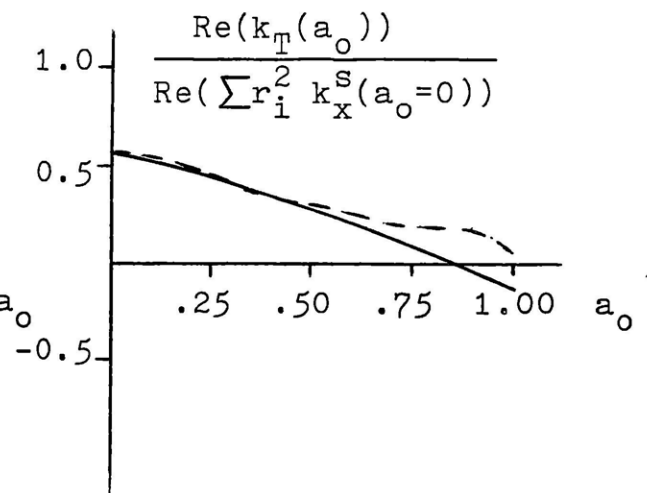
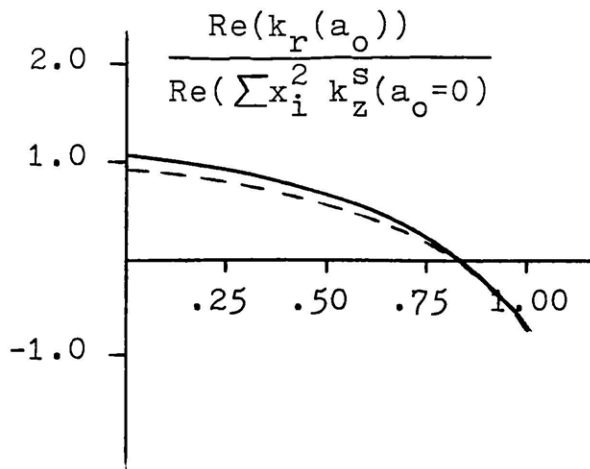


Figure 4.5
 Rocking Dynamic Stiffness
 of 4 x 4 Pile Group
 Solid Line - Kaynia

Figure 4.6
 Torsional Dynamic Stiffness
 of 4 x 4 Pile Group
 Solid Line - Kaynia

N = total number of piles in the group
(=16)

These figures show a good correlation with the results obtained using continuum theory by Kaynia, and serve to verify the validity of the present approach.

4.2.2 Embedded versus Non-Embedded Pile Foundations

Two of the advantages of the method formulated here are that a large number of piles may be analyzed very efficiently and that an embedded pile foundation may be analyzed. With these advantages in mind the effect of embedment is investigated using a system which is compatible with that of a nuclear containment structure.

The finite element mesh analyzed here for the embedded case is shown in figure 4.7 and for the non-embedded case in 4.8 with the material properties listed in table 4.1. Note that the non-embedded case is the same as the embedded case, with the soil above the elevation of the pile cap removed, and that the piles have pinned connections to the pile cap. Figure 4.9 shows the plan view of the pile layout. Note that the 185 piles are represented in the finite element mesh as only six pile rings.

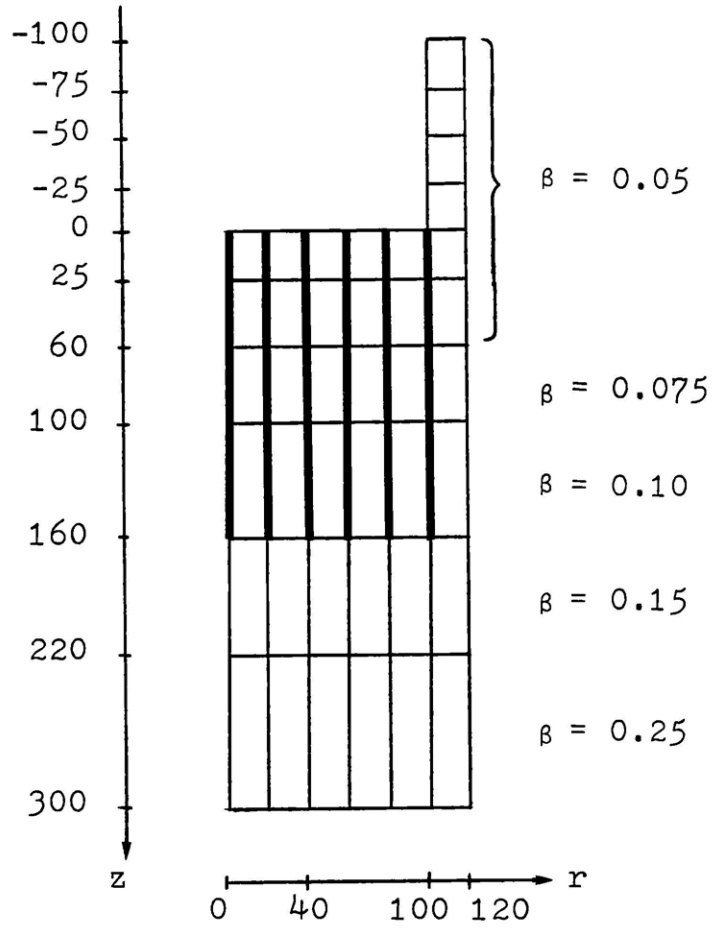


Figure 4.7
Finite element
mesh used for
embedded case

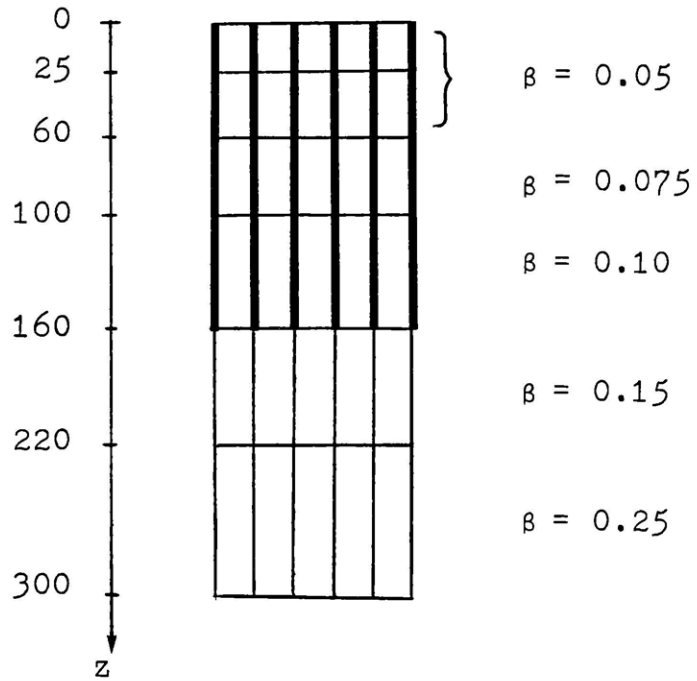


Figure 4.8
Finite element
mesh used for
non- embedded
case

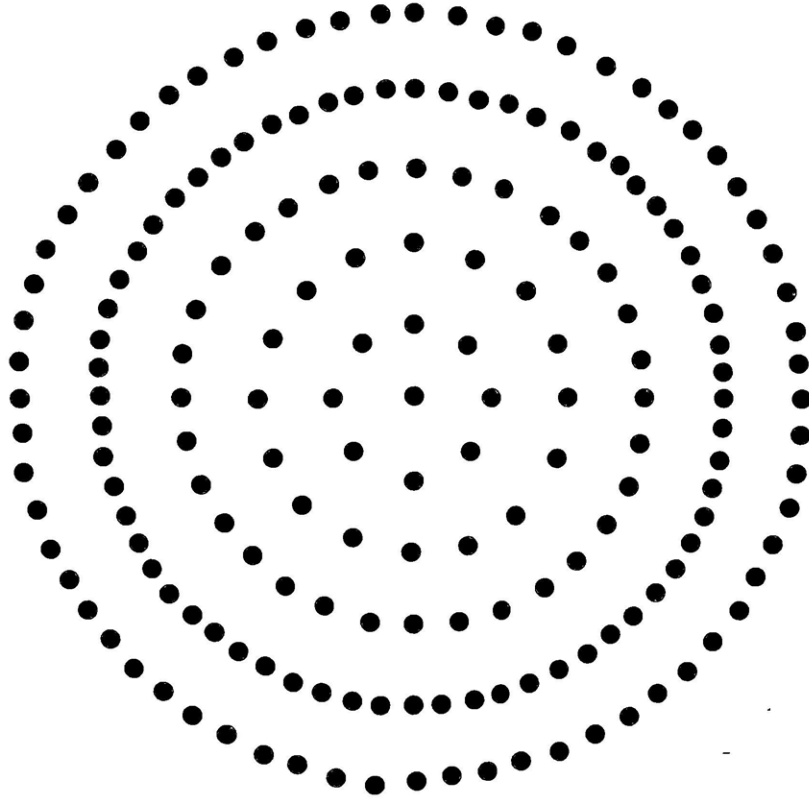


Figure 4.9
Pile Plan

PROPERTY	SOIL	PILE
γ	125 pcf	150 pcf
C_s	300 fps	-
ν	0.40	0.40
G	350 ksf	350×10^3 ksf
E	980 ksf	980×10^3 ksf
d	-	2 ft.

Table 4.1
Material Properties

Pile Ring	1	2	3	4	5	6
No. of piles in ring	1	8	16	32	64	64

Table 4.2
Pile Ring Information

Mode of Excitation	Embedded Stiffness (K_e)	Non-embedded Stiffness (K_n)
Vertical	9.088×10^8	8.226×10^8
Horizontal	3.439×10^8	2.286×10^8
Torsional	3.444×10^{12}	2.109×10^{12}
Rocking	5.740×10^{12}	4.907×10^{12}

Table 4.3
Static Stiffnesses

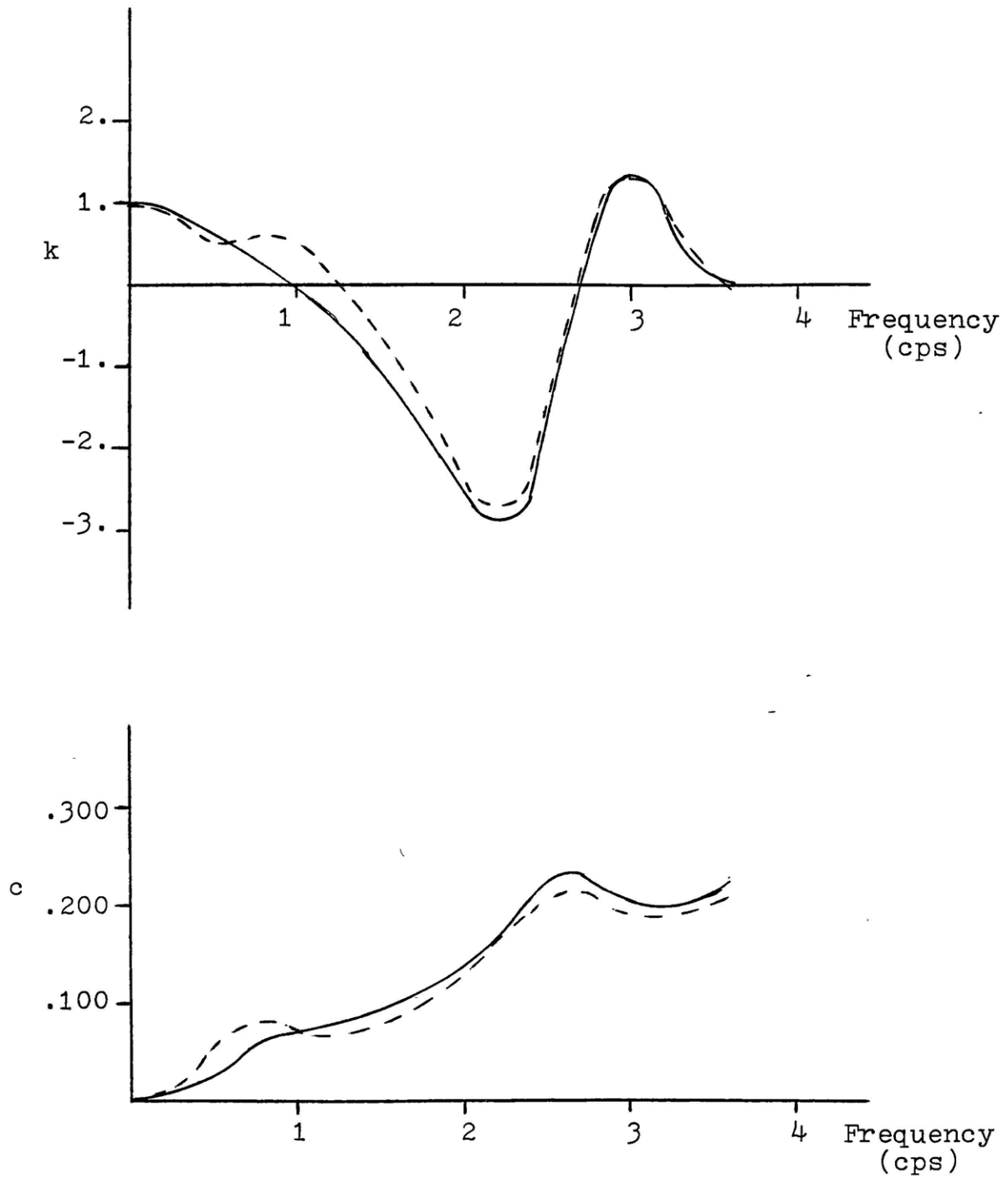


Figure 4.10
Dynamic stiffness coefficients for
vertical excitation
Solid Line - $E/R = 0.0$
Broken Line - $E/R = 1.0$

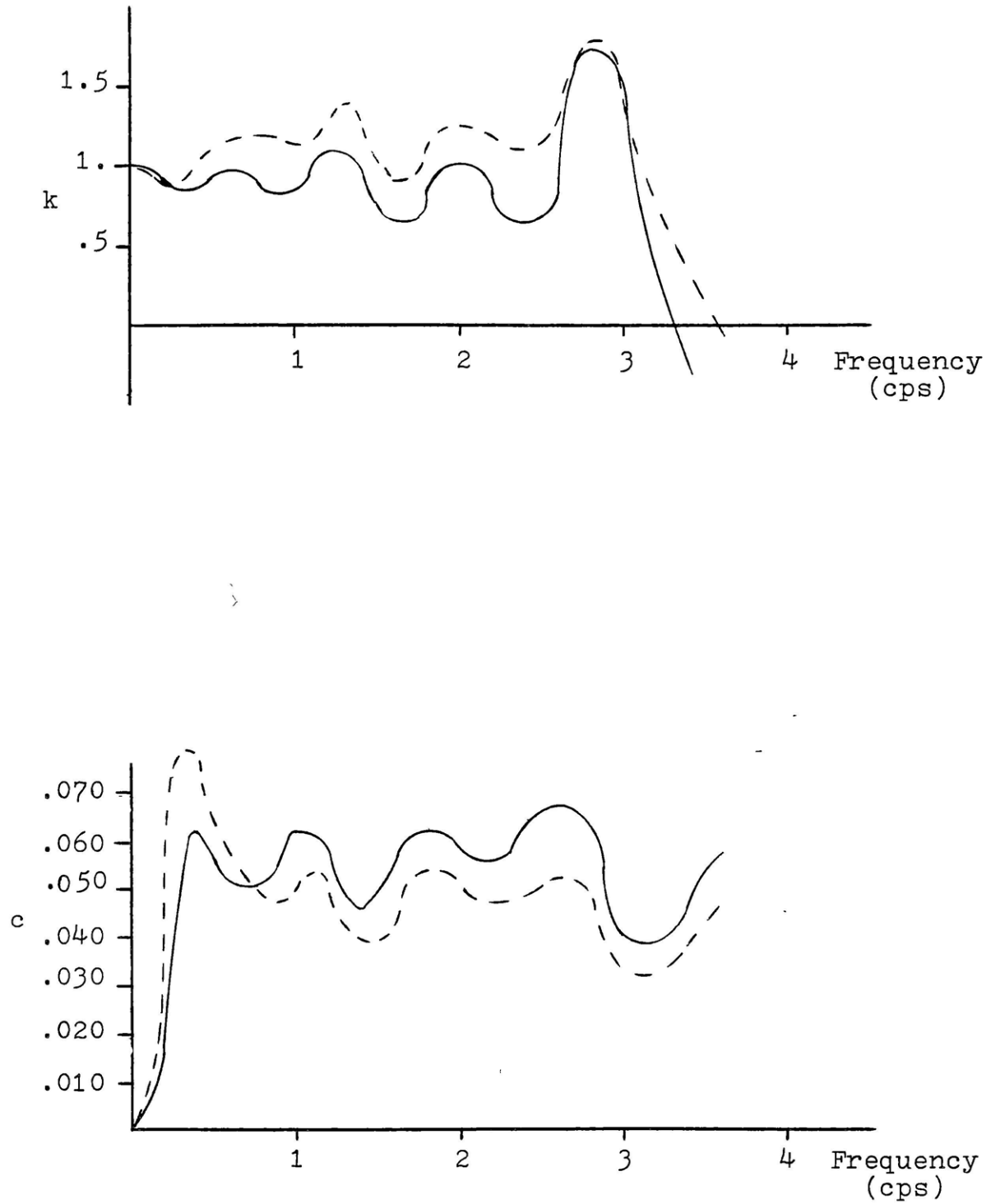


Figure 4.11
Dynamic stiffness coefficients for
horizontal excitation
Solid Line - $E/R = 0.0$
Broken Line - $E/R = 1.0$

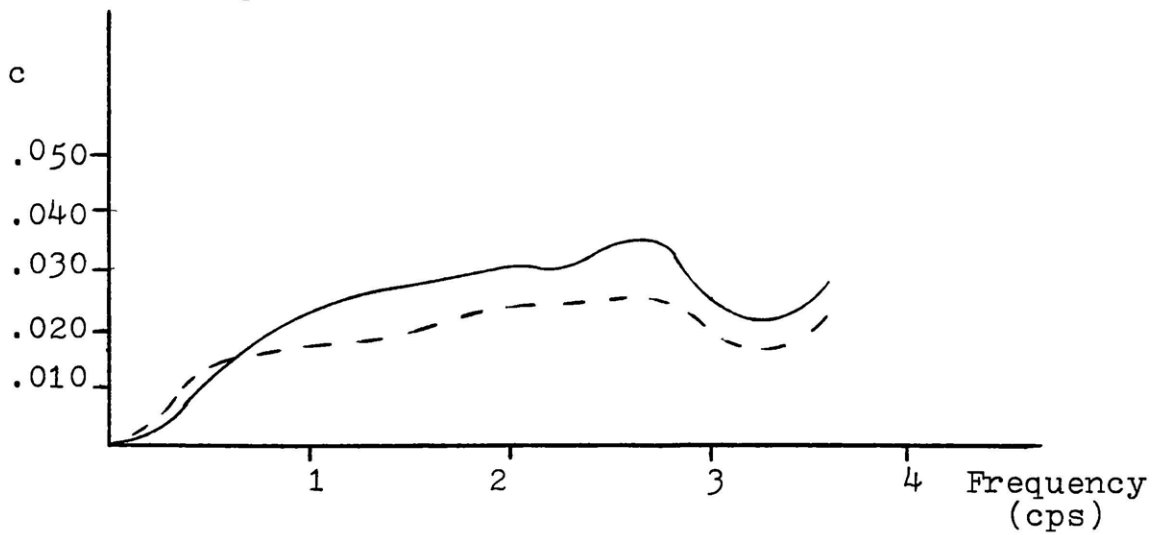
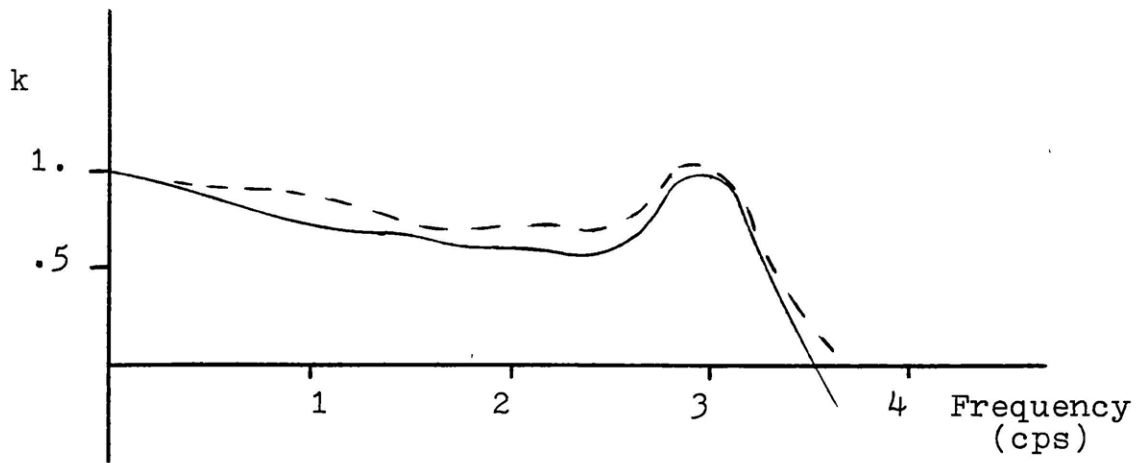


Figure 4.12

Dynamic stiffness coefficients for
torsional excitation

Solid Line - $E/R = 0.0$

Broken Line - $E/R = 1.0$

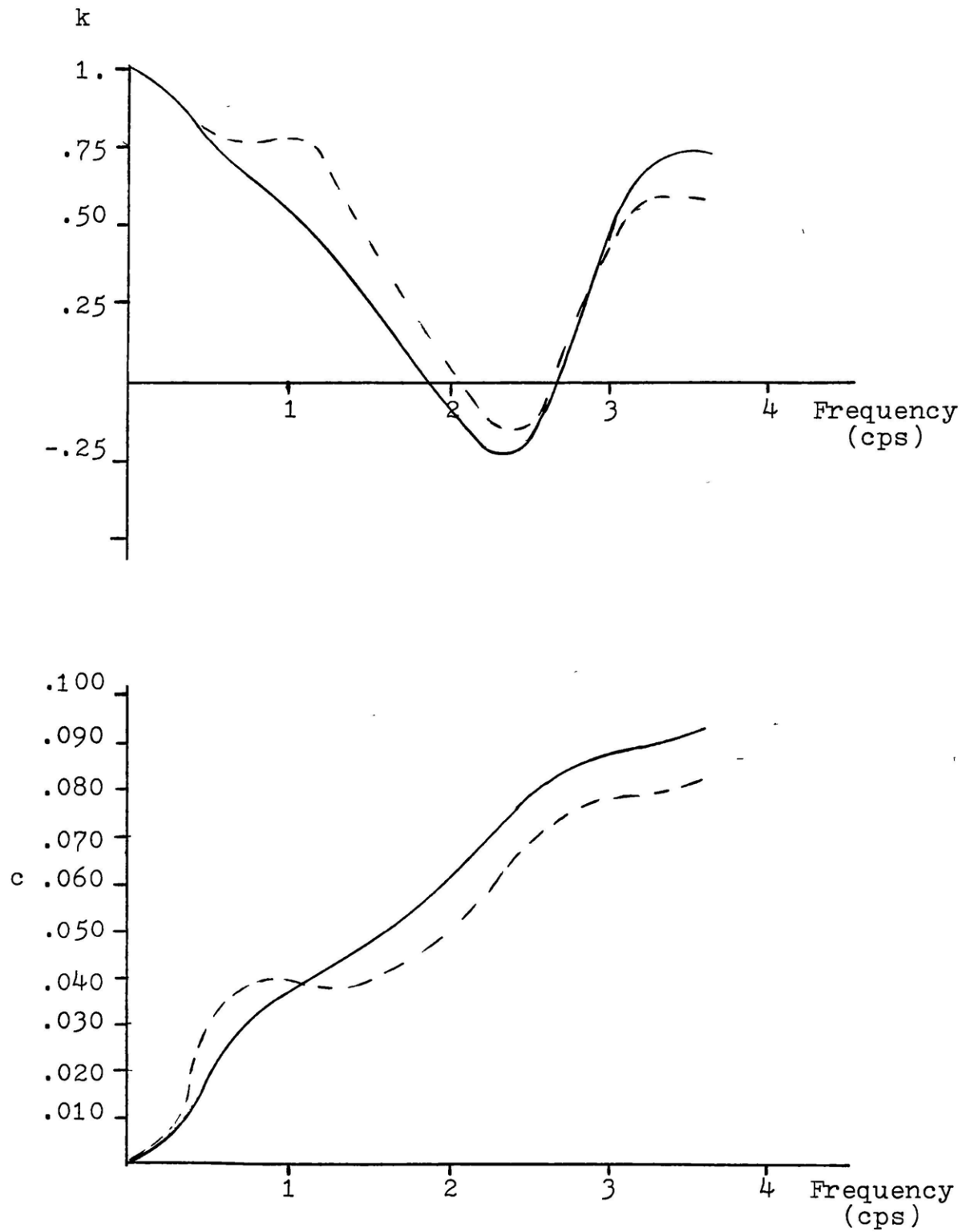


Figure 4.13
 Dynamic stiffness coefficients for
 rocking excitation
 Solid Line - $E/R = 0.0$
 Broken Line - $E/R = 1.0$

The variation of stiffness with frequency are presented for both embedded and non-embedded cases in figures 4.10 through 4.13 for vertical, horizontal, torsional and rocking stiffnesses, while the static stiffnesses are presented in table 4.3.

The static values for vertical and rocking stiffnesses increase by 10.5 and 17.0 percent, respectively, as a result of the embedment, while the corresponding increases for horizontal and torsional stiffnesses are 50.4 and 63.3 percent, respectively. This seems reasonable based on the idea of the confining effect the overburden soil has on the peripheral piles. The horizontal stiffnesses of the peripheral piles are increased more than the vertical stiffnesses. Therefore, the horizontal and torsional stiffnesses of the pile group, which mobilize the horizontal stiffness of the peripheral piles, increase more than the vertical and rocking stiffnesses.

In figures 4.10 through 4.13 the stiffness coefficients k and c are:

$$k = \text{Re} \left(\frac{K(\omega)}{K(0)} \right)$$

$$c = \frac{1}{a_0} \text{Im} \left(\frac{K(\omega)}{K(0)} \right)$$

where $K(\omega)$ is the complex stiffness at frequency ω , $K(0)$ is the complex static stiffness and

$$a_o = \frac{\omega R}{C_s}$$

where R is the radius of the cylindric foundation.

It is evident from these figures that the variation of stiffness with frequency, for each mode of excitation, is essentially the same for both embedded and non-embedded pile foundations. It can be seen that the real part (k) is generally slightly higher and the complex part (c) is slightly smaller for the embedded case than for the non-embedded case for each mode of excitation.

It is important for the use of these values to know that both the real (k) and complex (c) parts of the stiffness are functions of the frequency of excitation and the material damping, although the effect of damping is usually neglected. The damping effect could be accounted for using the correspondence principle if necessary. The complex term in the stiffness function (c) is related to the loss of energy to the system as a result of travelling waves. This effect is referred to as radiation damping.

4.3 Seismic Response of Pile Groups

When determining the motion of the foundation (kinematic interaction step of the foundation-structure analysis) it is useful to look at the transfer function for the acceleration of the pile cap. Figure 4.14 presents these transfer functions for the embedded and non-embedded cases subject to a horizontal excitation at the free surface, while figure 4.15 shows the phase angle. It is obvious that for the unembedded case the pile cap responds essentially the same as the free surface, while the embedded case behaves differently, filtering out some of the frequencies around six cycles per second but very little elsewhere. It may well be that the transfer function for the embedded case is determined more by the embedment than by the response of the pile group. Therefore, any conclusions regarding the response of embedded pile groups based on transfer functions must be the result of further study.

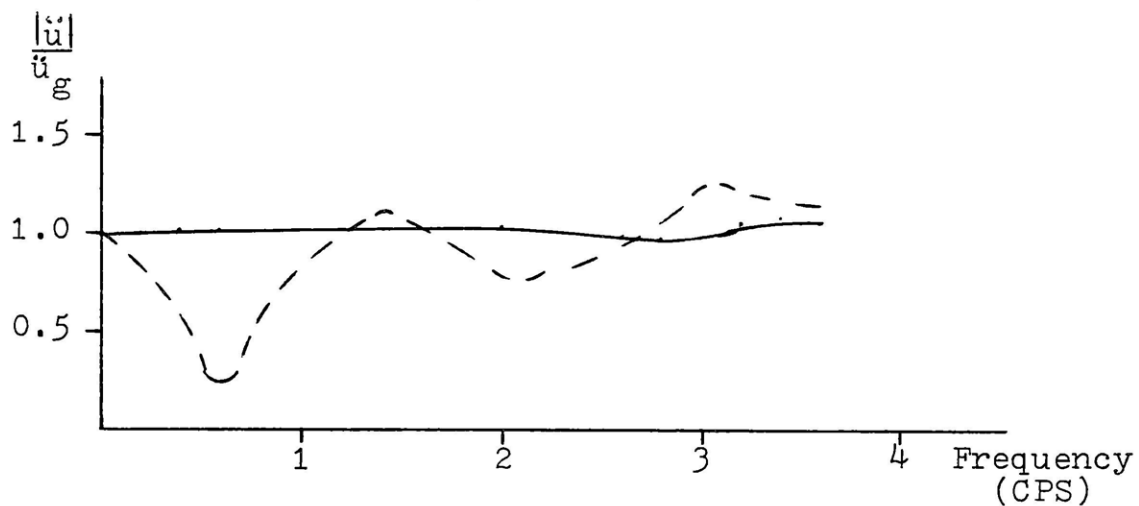


Figure 4.14
 Transfer Functions
 Solid Line - $E/R = 0.0$
 Broken Line - $E/R = 1.0$

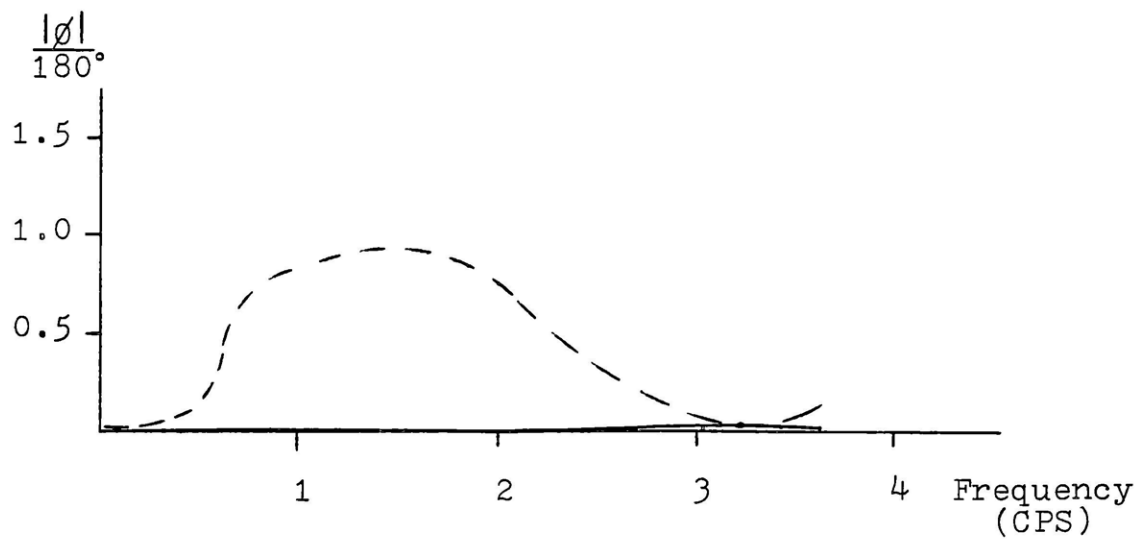


Figure 4.15
 Phase Angles
 Solid Line - $E/R = 0.0$
 Broken Line - $E/R = 1.0$

Chapter 5 - Conclusions

An approximate method of analysis has been developed for the dynamic analysis of axisymmetric pile groups. This method assumes that the displacement components for the piles in each ring may be described by Fourier series in the azimuth, an assumption that parallels the techniques used for solids of revolution, and results in a very efficient solution for the problem at hand.

The formulation has been implemented into a previously developed program for the analysis of cylindrical foundations embedded in layered media, based on a finite element formulation.

Verification of the numerical solution scheme was achieved using a 4 x 4 pile group case presented by Kaynia (8) who used three-dimensional continuum theory. The agreement between the two methods was quite good.

Dynamic analyses were performed on both an embedded and non-embedded soil-pile group profile that is compatible with that of a nuclear containment structure. The system analyzed had 185 piles which were distributed among six rings as an illustration of the efficiency of

the approach. The analysis revealed that while the embedded pile group had greater stiffness than the non-embedded case, the variation of stiffness with the frequency of excitation was essentially the same with both cases. The horizontal and torsional stiffness had a greater increase from the non-embedded case to the embedded case than did the vertical and rocking stiffnesses. This is due to the fact that the overburden, in the embedded case, confines the peripheral piles more to horizontal motions than to vertical motions.

APPENDIX A

Pile Element Stiffnesses

A.1 Introduction

For the implementation of the method formulated in this thesis it is desired to use the complete stiffness matrix for a pile element (fig. A.1) including axial, bending and shear effects, with consideration given to nonlinear axial effects. This appendix presents the derivation of this complete stiffness matrix using the consistent geometric stiffness matrix to account for the nonlinear axial effect.

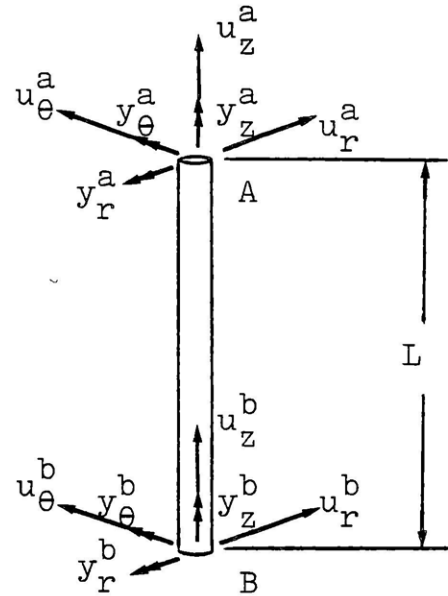


Figure A.1

Pile Element
Sign Convention

A.2 Stiffness Matrix

The combined general stiffness matrix for an element equals the elastic stiffness matrix (ref. Clough and Penzien)

$$\bar{K} = K - K_g .$$

The elastic stiffness matrix, K , is derived below for bending and shear effects. Later the consistent geometric

stiffness matrix is presented, and the combined general stiffness matrix is given in its final form.

A.3 Determination of Elastic Stiffness Matrix

From beam theory we know

$$dM = -Vdx .$$

Integrating once, assuming the shear, V , is constant we get

$$M = -Vx + c_1 \quad (A.1)$$

Dividing the bending moment, M , by the flexural rigidity, EI , and integrating yields

$$dy = \frac{1}{EI} \left(\frac{-Vx^2}{2} + c_1x \right) + c_2 \quad (A.2)$$

The deflection of a pile or beam element considering both shear and bending is given by

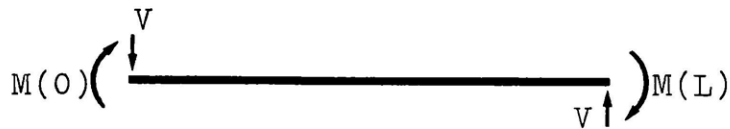
$$y = \int dydx + \lambda \frac{Vx}{GA}$$

where λ is a shape factor that depends on the geometry of the cross section ($\lambda = 7/6$ for circular cross sections). Evaluating the integral results in a final expression for the deflection

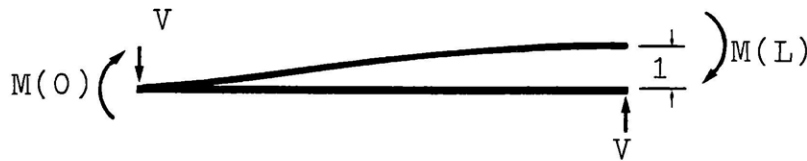
$$y = \frac{1}{EI} \left(\frac{-Vx^3}{6} + \frac{c_1x^2}{2} \right) + c_2x + c_3 + \lambda \frac{Vx}{GA} \quad (A.3)$$

The stiffness coefficients for the pile element are found by specifying certain boundary conditions on the elements and solving equations A.1 through A.3 for the three constants of integration. The stiffness coefficients then correspond to the end forces required to cause the given boundary conditions.

When evaluating the boundary value problems the following sign convention is used:



Condition 1:



Boundary Conditions:

$$y(0) = 0$$

$$y(L) = 1$$

$$dy(0) = 0$$

$$dy(L) = 0$$

Constants of Integration:

$$c_1 = \frac{VL}{2}$$

$$c_2 = c_3 = 0$$

End Loads:

$$V = \left(\frac{L^3}{12EI} + \frac{\lambda L}{GA} \right)^{-1}$$

$$M(0) = \frac{L}{2} \left(\frac{L^3}{12EI} + \frac{\lambda L}{GA} \right)^{-1} \quad (\text{A.4b})$$

$$M(L) = -\frac{L}{2} \left(\frac{L^3}{12EI} + \frac{\lambda L}{GA} \right)^{-1} \quad (\text{A.4c})$$

Condition 2:



Boundary Conditions:

$$y(0) = 0 \quad y(L) = 0$$

$$dy(0) = 0 \quad dy(L) = 1$$

Constants of Integration:

$$c_1 = \frac{EI}{L} + \frac{VL}{2}$$

$$c_2 = c_3 = 0$$

End Loads:

$$V = -\frac{L}{2} \left(\frac{L^3}{12EI} + \frac{\lambda L}{GA} \right)^{-1} \quad (\text{A.5a})$$

$$M(0) = \frac{EI}{L} - \frac{L}{4} \left(\frac{L^3}{12EI} + \frac{\lambda L}{GA} \right)^{-1} \quad (\text{A.5b})$$

$$M(L) = \frac{EI}{L} + \frac{L}{4} \left(\frac{L^3}{12EI} + \frac{\lambda L}{GA} \right)^{-1} \quad (\text{A.5c})$$

The elastic stiffness matrix for the pile element using the sign convention presented in figure A.1 is as

follows:

$$\begin{Bmatrix} v_{rr}^a \\ M_{\theta}^a \\ v_{rr}^b \\ M_{\theta}^b \end{Bmatrix} = \begin{bmatrix} K_{aa} & K_{ab} \\ K_{ba} & K_{bb} \end{bmatrix} \begin{Bmatrix} u_{rr}^a \\ y_{\theta}^a \\ u_{rr}^b \\ y_{\theta}^b \end{Bmatrix} \quad (\text{A.6a})$$

$$\begin{Bmatrix} v_{\theta}^a \\ M_{rr}^a \\ v_{\theta}^b \\ M_r^b \end{Bmatrix} = \begin{bmatrix} K_{aa} & K_{ab} \\ K_{ba} & K_{bb} \end{bmatrix} \begin{Bmatrix} u_{\theta}^a \\ y_{rr}^a \\ u_{\theta}^b \\ y_r^b \end{Bmatrix} \quad (\text{A.6b})$$

$$\begin{Bmatrix} v_z^a \\ v_z^b \end{Bmatrix} = \frac{EA}{L} \begin{bmatrix} 1 & -1 \\ -1 & 1 \end{bmatrix} \begin{Bmatrix} u_z^a \\ u_z^b \end{Bmatrix} \quad (\text{A.6c})$$

$$\begin{Bmatrix} M_z^a \\ M_z^b \end{Bmatrix} = \frac{GJ}{L} \begin{bmatrix} 1 & -1 \\ -1 & 1 \end{bmatrix} \begin{Bmatrix} y_z^a \\ y_z^b \end{Bmatrix} \quad (\text{A.6d})$$

where

$$K_{aa} = \begin{bmatrix} v' & -\frac{L}{2} v' \\ -\frac{L}{2} v' & \frac{EI}{L} + \frac{L^2}{4} v' \end{bmatrix}$$

$$K_{ab} = K_{ba}^T = \begin{bmatrix} -v' & -\frac{L}{2} v' \\ \frac{L}{2} v' & -\frac{EI}{L} + \frac{L^2}{4} v' \end{bmatrix}$$

$$K_{bb} = \begin{bmatrix} v' & \frac{L}{2} v' \\ \frac{L}{2} v' & \frac{EI}{L} + \frac{L^2}{4} v' \end{bmatrix}$$

and

$$v' = \left(\frac{L^3}{12EI} + \frac{\lambda L}{GA} \right)^{-1} .$$

Note that when the shear term in v' is removed the stiffness matrix reduces to the well known stiffness matrix ignoring shear deformations.

A.4 Consistent Geometric Stiffness Matrix

The geometric stiffness matrix provides consideration for the force component acting in the same direction as the original axis of the element, leading to additional load components in the direction of the nodal displacements. The element of the geometric stiffness matrix $k_g(i,j)$ is equal to the force corresponding to degree of freedom i due to a unit displacement of degree of freedom j , resulting from the axial force component in the element.

The consistent geometric stiffness matrix for the pile element corresponds to equations A.6, where

$$K_{g_{aa}} = \begin{bmatrix} \frac{6P}{5L} & \frac{-P}{10} \\ \frac{-P}{10} & \frac{4}{30} PL \end{bmatrix}$$

$$K_{g_{ab}} = K_{g_{ba}}^T = \begin{bmatrix} -\frac{6P}{5L} & -\frac{P}{10} \\ \frac{P}{10} & \frac{PL}{30} \end{bmatrix}$$

$$K_{g_{bb}} = \begin{bmatrix} \frac{6P}{5L} & \frac{P}{10} \\ \frac{P}{10} & \frac{4}{30} PL \end{bmatrix}$$

A.5 Combined General Stiffness Matrix

The final combined stiffness matrix equals the elastic stiffness matrix minus the geometric stiffness matrix. The final matrix is in the form of equations A.6 where

$$K_{aa} = \begin{bmatrix} v' - \frac{6P}{5L} & -\frac{L}{2}v' + \frac{P}{10} \\ -\frac{L}{2}v' + \frac{P}{10} & \frac{EI}{L} + \frac{L^2}{4}v' - \frac{4}{30}PL \end{bmatrix}$$

$$K_{ab} = K_{ba}^T = \begin{bmatrix} -v' + \frac{6P}{5L} & -\frac{L}{2}v' + \frac{P}{10} \\ \frac{L}{2} - \frac{P}{10} & -\frac{EI}{L} + \frac{L^2}{4} + \frac{1}{30}PL \end{bmatrix}$$

$$K_{bb} = \begin{bmatrix} v' - \frac{6P}{5L} & \frac{L}{2}v' - \frac{P}{10} \\ \frac{L}{2}v' - \frac{P}{10} & \frac{EI}{L} + \frac{L^2}{4}v' - \frac{4}{30}PL \end{bmatrix}$$

BIBLIOGRAPHY

1. Apsel, R., "Dynamic Green's Functions for Layered Media and Applications to Boundary-Value Problems," Ph.D. Thesis submitted to the Department of Applied Mechanics and Engineering Sciences, University of California, San Diego, 1979.
2. Banerjee, P.K., "Analysis of Axially and Laterally Loaded Pile Groups," in Developments in Soil Mechanics, Ed., C.E. Scott, Chapter 9, Applied Science Publishers, London, 1978.
3. Banerjee, P.K. and Driscoll, P.M., "Three-dimensional Analysis of Raked Pile Groups," Proc. Instn. Civ. Engrs., Part 2, Vol. 61: 643-671, 1978.
4. Clough, R.W. and Penzien, J., Dynamic of Structures, McGraw-Hill, 1975.
5. Kausel, Eduardo, "Forced Vibrations of Circular Foundations on Layered Media," Research Report R74-11, M.I.T. Department of Civil Engineering, Cambridge, Massachusetts, January 1974.
6. Kausel, Eduardo, "An Explicit Solution for the Green Functions for Dynamic Loads in Layered Media," Research Report R81-13, M.I.T. Department of Civil Engineering, Cambridge, Massachusetts, May 1981.
7. Kausel, E. and Ushijima, R., "Vertical and Torsional Stiffnesses of Cylindrical Footings," Research Report R79-6, M.I.T. Department of Civil Engineering, Cambridge, Massachusetts, February 1979.
8. Kaynia, A.M., "Dynamic Stiffnesses and Seismic Response of Pile Groups," Research Report R82-03, M.I.T. Department of Civil Engineering, Cambridge, Massachusetts, January 1982.
9. Nogami, T., "Dynamic Group Effect of Multiple Piles under Vertical Vibration," Proc. of ASCE Engineering Mechanics Specialty Conference, Austin, Texas, 1979.
10. Nogami, T., "Dynamic Stiffnesses and Damping of Pile Groups in Inhomogeneous Soil," ASCE special technical publication on Dynamic Response of Pile Foundations, October 1980.

11. Poulos, H.G., "Analysis of the Settlement of Pile Groups," Geotechnique, Vol. 18, 1968, pp. 449-471.
12. Poulos, H.G., "Behavior of Laterally-Loaded Piles: II-Pile Groups," Journal of the Soil Mechanics and Foundation Division, ASCE, Vol. 97, No. SM5, 1971, pp. 733-751.
13. Poulos, H.G. and Davis, E.H., "Pile Foundation Analysis and Design," John Wiley and Sons, New York, N.Y., 1980.
14. Waas, G. and Hartman, H.G., " Analysis of Pile Foundations under Dynamic Loads," SMIRT Conference, Paris, 1981.
15. Wolf, J.P. and Von Arx, G.A., "Impedance Function of a Group of Vertical Piles," Proc. of the ASCE Geotechnical Engineering Division, Specialty Conference on Earthquake Engineering and Soil Dynamics, Pasadena, California, 1978, pp. 1024-1041.